APPLICATION OF CAPILLARY PRESSURE TO LOG ANALYSIS

by

John H. Doveton

Kansas Geological Survey
Open-file Report 99-53

Kansas Geological Survey
1930 Constant Avenue
University of Kansas
Lawrence, KS 66047-3726

Application of capillary pressure to log analysis

By John H. Doveton

1999

HYDROCARBON RESERVOIR STRUCTURE, PERMEABILITY, FLUID SATURATION AND PRODUCTION

The illustration on the next page is a schematic representation of a simple, homogeneous reservoir that was originally completely water saturated (and water-wet). Migrating oil (and/or gas) has completely filled the anticlinal structure above the spill-point. The free-water level (FWL) coincides with the spill-point in this example because the trap is completely charged. Notice that the FWL does not coincide with the oil-water contact (OWC), regardless whether the OWC is defined as the deepest zone that will flow oil (as well as water) or the maximum depth at which the formation will produce oil with no water-cut (the definition of OWC used in this course).

The controls for the fluid distributions and fluid production in this reservoir are found in the equilibrium between the buoyancy pressure exerted by the lighter hydrocarbons moving upwards and the resistance exerted by capillary forces that hold the wetting phase of formation water to the pore surfaces. As they move upwards, the obstacles to the movement of the of oil globules are presented by the constrictions of the pore throats, rather than the pores themselves. Large pore throats are obviously penetrated more easily than small pore throats. A rock with uniform and enormous pore throats would be permeated completely throughout the entire height of the reservoir ; the OWC would coincide with the FWL, and there would be no transition zone.

A conventional rock has a distribution of pore throat sizes that will be penetrated at various levels above the FWL as the buoyancy pressure increases and penetrates progressively smaller pore throats. Immediately above the FWL, the buoyancy pressure is very low, so that only the large pore throats are breached. The majority of pores are still completely filled with water. At this level, the well-site geologist might well notice some minor oil-stain in the sample. Core samples would also show low oil saturations. However, if a test were made the produced sample would be entirely water. The oil stays in the rock as isolated globules and constitutes "residual oil saturation", Sor.

Moving higher above the FWL the produced fluid would change from water to water with a small oil-cut. This point marks the bottom of the transition zone and occurs when the increased buoyancy pressure causes a more pervasive penetration of pore throats to the point that oil globules have started to form continuous filaments through the pore network. The continuity of the oil phase now allows it to flow together with the water. At still shallower depths, the oil cut becomes greater until fluid production shifts to recoveries of water-cut oil. Finally, a depth is reached when no water-free oil is produced and marks the lower boundary of the reservoir zone. The remaining water is immobile for Darcian fluid flow and is found as thin films on pore surfaces, within micropores, and, possibly, finer macropores. At still higher levels, all the macropores are filled and the remaining water is contained within the micropores as "irreducible" water.

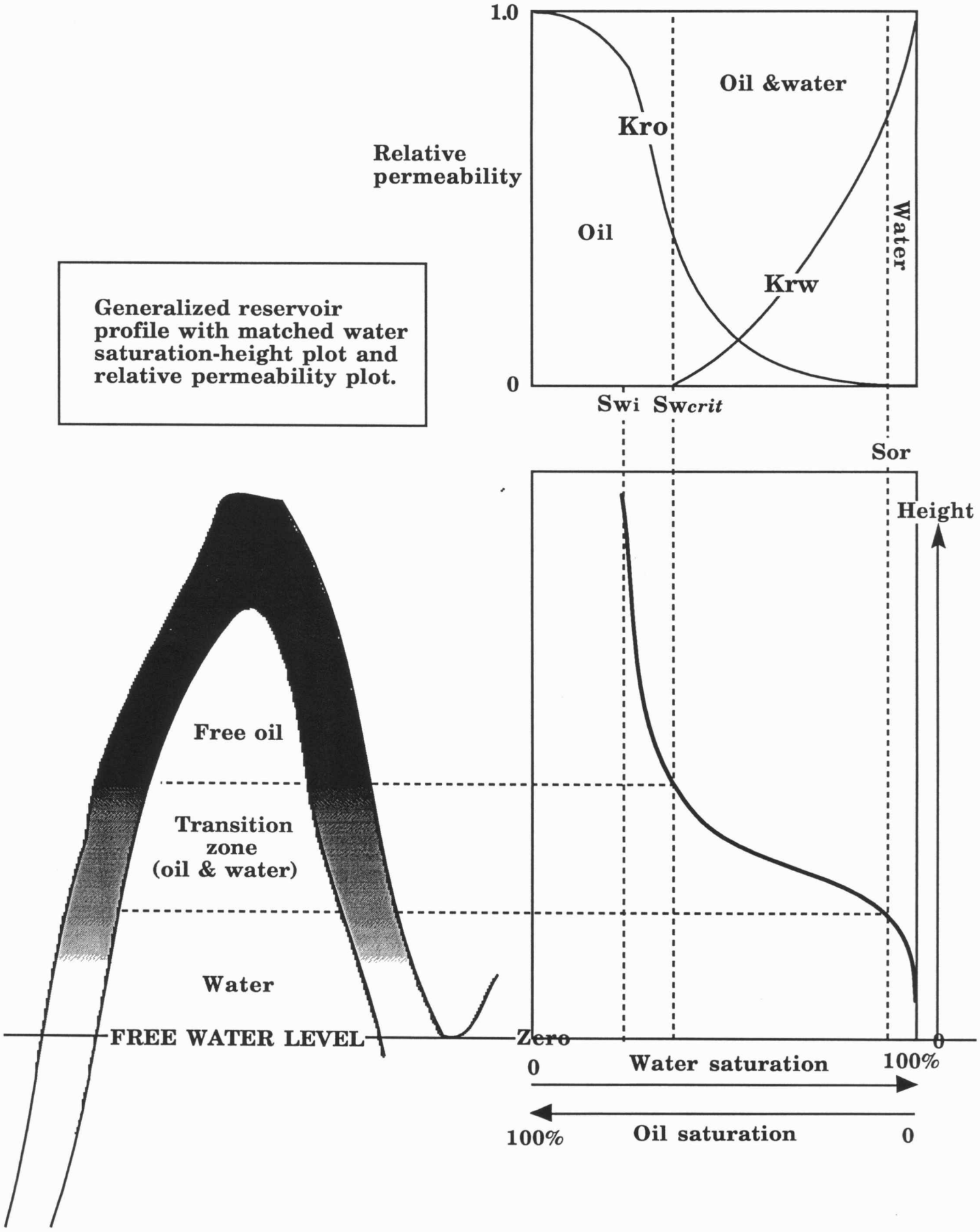

Generalized reservoir profile with matched water saturation-height plot and relative permeability plot.

The fluid production performance of this reservoir profile is captured by the relative permeabilities of the reservoir rock with respect to oil and water as a function of fluid saturations. Simple concepts of permeability consider the situation where a rock has a single fluid, typically water, and the permeability measured is then the "absolute permeability", *K*. With two (or more) phases the ability of a fluid to flow is now not only controlled by the pore network, but the distribution of the other phases within the pores. For an oil /water system, two relative permeabilities can be defined and symbolized by *Kro* and *Krw*. Their values are determined by the ratio of the permeability of the phase to the absolute permeability of the rock for a single fluid.

Between the FWL and the base of the transition zone, the isolated globules of oil are not produced and the relative permeability to oil, *Kro.* is essentially zero. Above the base of the transition zone, *Kro* increases progressively and moves asymptotically to unit value (equivalence with absolute permeability) as the water phase becomes immobile and confined to progressively smaller pores.

The relative permeability to water, *Krw*, is clearly equal to unity at the Free-Water Level where the rock contains water as its only phase. Above the FWL, *Krw* declines as the oil saturation increases until a "critical water saturation", *Swcrit*, is reached, when Krw is effectively zero. This saturation marks the oil-water contact above which no water production occurs. Notice that *Swcrit* is different from *Swi* (although they can be coincident in some rocks). The irreducible water saturation, *Swi*, marks immobile water held in micropores. *Swi* is often approximately constant over moderate heights of uniform reservoir rock, basically because many rocks (particularly clastics) have a distinctly bimodal macropore/micropore system. The relatively lower frequencies of pore throat sizes between the two categories causes a relatively stable value of water saturation until sufficient height of hydrocarbon column is attained to penetrate the larger micropores. However, Swcrit takes a larger value than *Swi* when some proportion of the smaller macropores fail to contribute any permeability for their contained water when all the larger pores are filled with oil. In the absence of any specific information, some log analysts use a rule-of-thumb that the critical water saturation is approximately equal to the square root of the irreducible water saturation : $Sw_{crit} = \sqrt{Sw_i}$. This would provide a very broad figure and estimates of *Swi* from core measurements of relative permeability should be used whenever they are available.

In summary, the fluid saturations and production are determined by:

(1) the oil or gas column height which, together with the density difference between the hydrocarbon and the formation water, controls the buoyancy pressures as they increase above the Free Water Level;

and (2) the pore throat sizes and their distributions within the formation rock. If the rock is dominated by large pore throats, the transition zone is minimal and the OWC is close to the FWL. If the rock is mostly made up of small pore throats

then the transition zone can become very long ; possibly longer than the closure of the trap, in which case, no water-free hydrocarbons can be produced. If the rocks are primarily very fine pores then the buoyancy pressure exerted by a potential oil or gas column may be insufficient to penetrate the pores and the rock is a seal ; by the same token, with a sufficiently large closure, this same "seal" may produce hydrocarbons, albeit above a very long transition zone.

This range of possible hydrocarbon column scenarios shows a basic limitation of the schematic reservoir used to illustrate points so far: this simple reservoir is composed of a single rock type with both a constant porosity and size range of pore throat sizes. In reality, a reservoir rock will often show gross lateral changes in facies across a field and rapid changes vertically that reflect the interbeddings of different petrofacies. If there is a lateral gradient to smaller pore-throat sizes, then the oil-water contact will actually rise in the field to give an apparent tilted contact, because the transition zone is lengthened. The illustration taken from Arps (1964) shows this phenomenon, together with the logs that would be expected for three wells in a hypothetical structural trap.

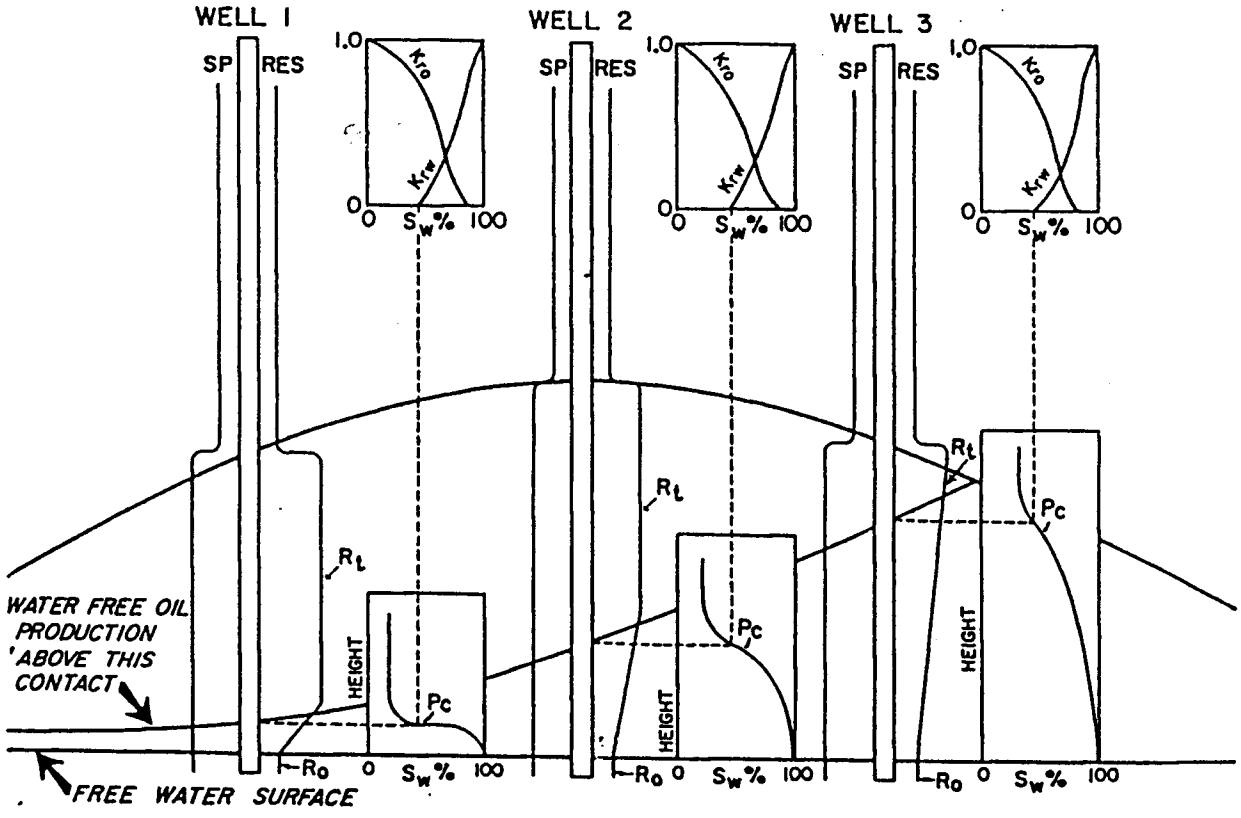

Tilted oil-water contact with changing rock characteristics (from Arps, 1964)

The model is borne out by observations in many fields, where sometimes puzzling shifts in oil-water contacts merely reflect facies changes in the reservoir rock. So, for example, Cuddy et al (1993) advocate the use of the FWL as a consistent datum in gas fields in the North Sea in preference to the Gas Water Contact, precisely because the GWC shows vertical shifts that reflect rock quality. In addition, lengthy transition zones have meant that "many equity determinations have foundered over arguments" concerning an appropriate water saturation criterion to determine the GWC.

In the vertical dimension, there will be an overall trend to decreasing water saturation moving upwards, but the trend will be broken by excursions to lower or higher saturations that reflect changes to larger or smaller permeabilities and pore-throat sizes. The exact pattern will be determined by the structure of the reservoir ; whether it is relatively homogeneous or whether it consists of layers of rock with distinctly different pore size distribution. Although the water saturation profile may be choppy, there will be many instances where the bulk volume water will be smoother, because higher water saturations will tend to be associated with lower porosities and vice-versa. Once the reservoir level is reached, the BVW becomes "irreducible" and has a value of the reservoir rock's Buckles number, *c*. Remember that *c* probably represents the fraction of the rock that consists of microporosity. We will consider a "petrofacies" to be defined as a rocktype which, while having variable total porosity, has essentially constant microporosity, and so, constant Buckles number. Of course, if the reservoir consists of several petrofacies, then the BVW will show significant fluctuations within the main reservoir.

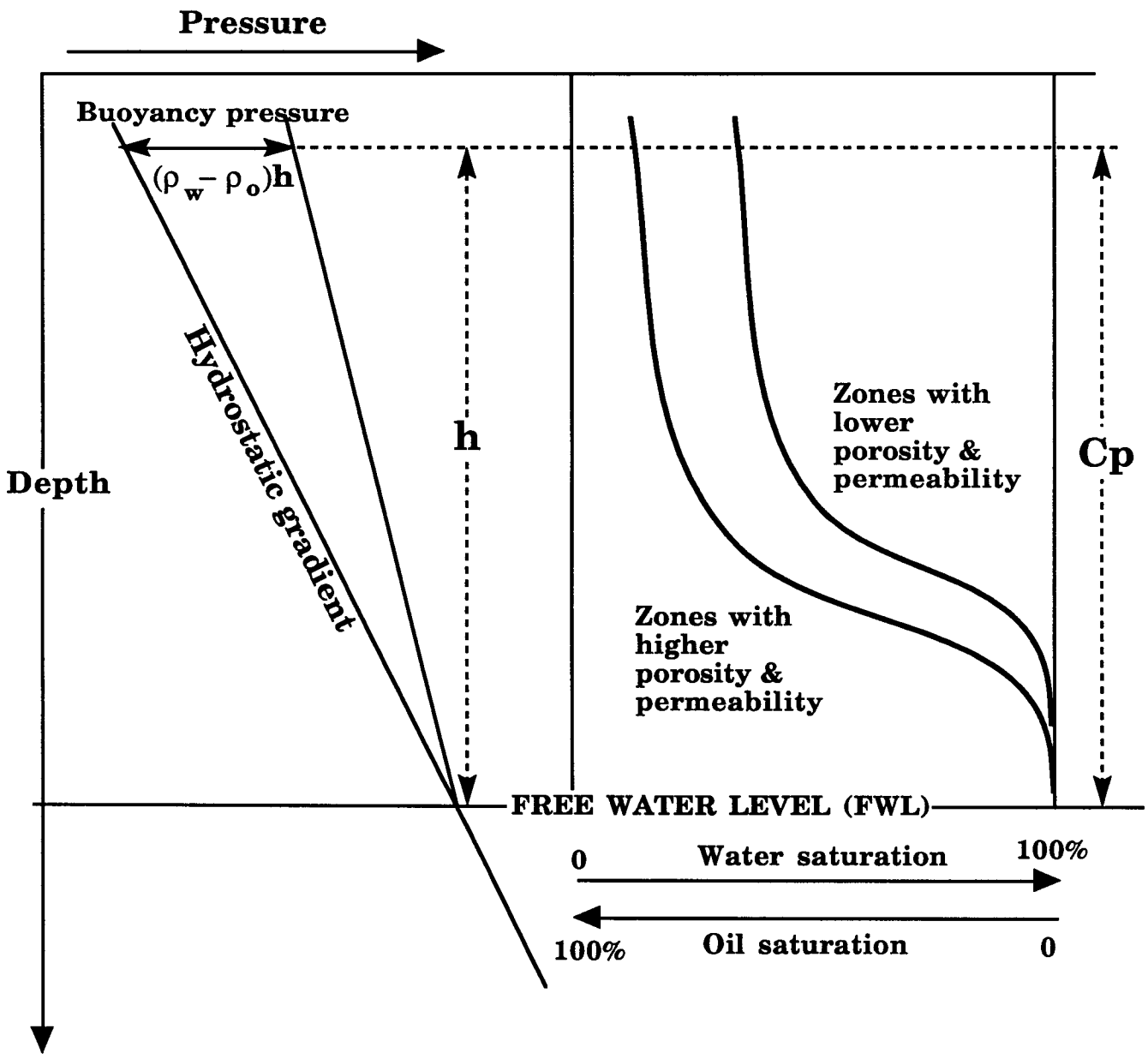

Relationship between buoyancy pressure (product of the hydrocarbon column, h, and the difference in density between formation water and hydrocarbon) and capillary pressure, Cp, as function of capillary forces that holds the wetting-phase of water in successively finer pores.

CAPILLARY PRESSURE MEASUREMENTS AND THEIR USE IN ESTIMATION OF PORE-THROAT SIZE AND LOCATION IN A HYDROCARBON COLUMN

Capillary pressure data have been obtained from core samples by the oil industry for about fifty years, but their primary users have been petroleum engineers. Fortunately, several excellent review papers have been written for geologists that relate capillary pressure to rock type and reservoir structure, as well as applications to both reservoir analysis and exploration (Arps, 1964; Stout, 1964; Berg, 1975; Jennings, 1987; Vavra et al, 1992).

Capillary pressure measurements are made on standard core plugs by injecting mercury at increasing pressures and recording the mercury saturation of the core at different pressure levels. The laboratory process simulates the intrusion of hydrocarbons into a water-wet rock under increasing buoyancy pressure that would be experienced by the rock at successively higher levels in a hydrocarbon column. A mercury/air system is routinely used in preference to a hydrocarbon and water, because the procedure is faster, easier, and cheaper ; conversions to any hydrocarbon/water system can be made through the use of equations that are described later.

Initially, the plug is placed in a capillary pressure chamber where the pressure is reduced to zero by application of a vacuum. The chamber is then filled with mercury and pressure increased by incremental steps. At each step, the core sample imbibes mercury and, when the process reaches equilibrium, the quantity of mercury that is needed to replenish the chamber is a measure that can be added to the sample cumulative mercury saturation recorded up to that pressure. A graph of a typical capillary pressure curve is shown on the next page and is indexed with some key descriptive features. The pressure is commonly recorded in "psi" (pounds per square inch) units that are used in this course, but the figure shows conversion factors to other units of atmospheres and kilograms per square centimeter.

The obstacle to the introduction of mercury into the core is provided by the capillary forces within the pore system. In a hydrocarbon system, the wetting fluid (conventionally thought to be water) adheres to the internal surfaces and resists the introduction of the hydrocarbon non-wetting phase. The equation of the capillary forces is given by:

$$Pc = \frac{2\sigma\cos\theta}{r}$$

where Pc is the capillary pressure, σ is the surface tension of the wetting fluid, θ is the contact angle between the wetting fluid and the solid surface and r is the pore throat radius. Because the term $2\sigma\cos\theta$ is a constant for any given non-wetting/wetting fluid (or gas) couplet, the capillary pressure is controlled by the pore throat radius of the rock pores. If the pore throats had a unique radius, then the pore network would be impenetrable up to a critical pressure, when the

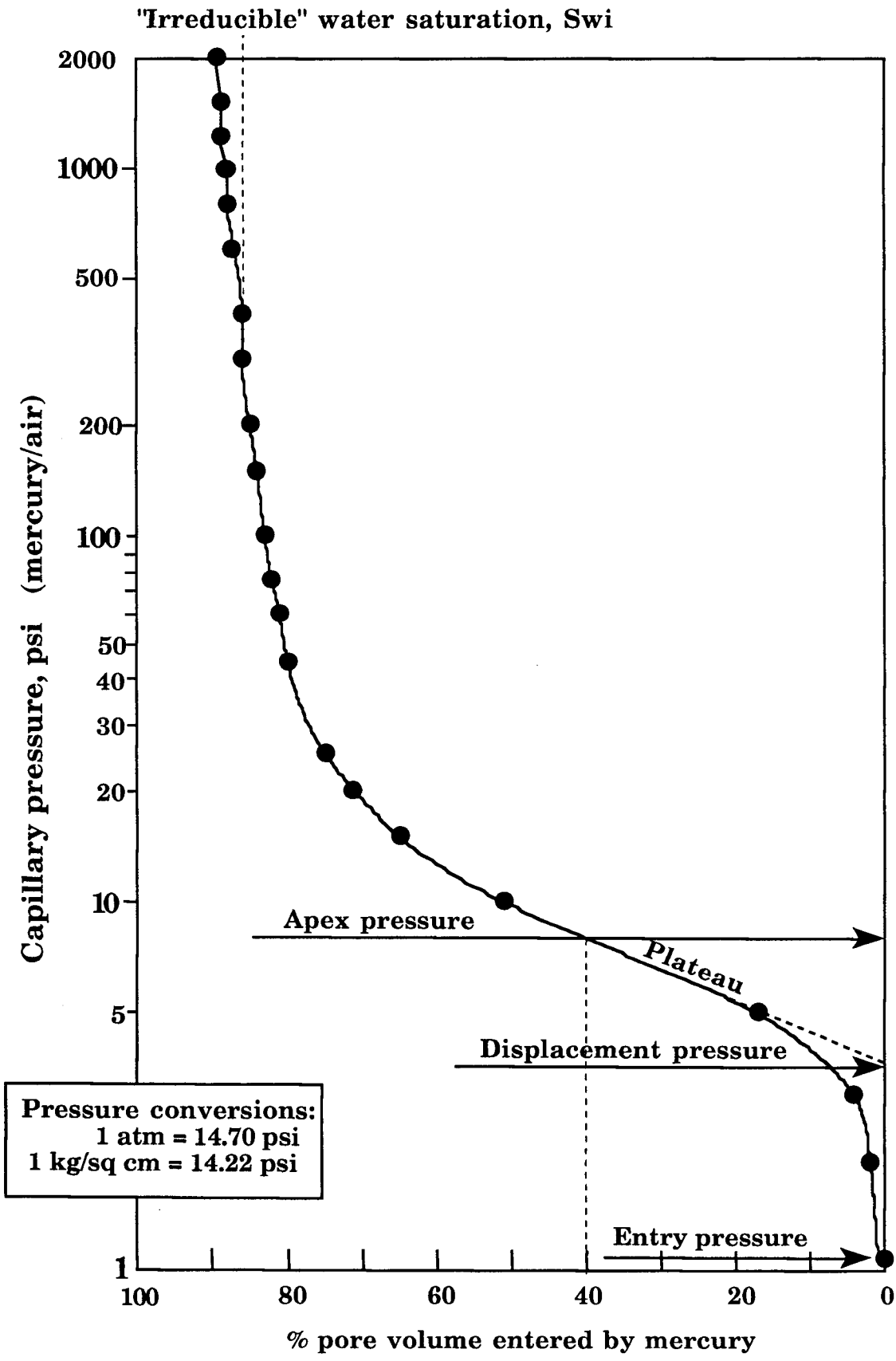

Major descriptive features of a typical capillary pressure curve.

entire pore system would be breached. In reality, rock pore systems have a range of pore throat sizes, so that the capillary pressure curve records the saturation of pore throats at successively smaller sizes with increasing pressure. The curve is a rendition of a cumulative frequency curve of pore throat sizes.

The pressure at which the core sample first imbibes mercury is called the *entry pressure*. This is generally not a particularly diagnostic feature, because sliced pores at the core surface create artificially large "pore throats" as a boundary effect. At increasing pressures, however, a point is generally reached when the sample imbibes mercury in a more systematic fashion and a trend is picked up by a "plateau" feature. The slope of the plateau reflects the overall pore-throat size distribution: if horizontal, then there is a narrow range of pore-throat sizes (they are "well-sorted"); if a steep slope, then there is a wide distribution (they are "poorly-sorted'). The extrapolation of the plateau to the pressure axis marks the *displacement pressure*, which is widely used as the (mercury) pressure at which hydrocarbons will enter the rock. (When converted to equivalent buoyancy pressure, this also gives the minimum hydrocarbon column necessary in a trap of this reservoir rock to allow entry by hydrocarbons).

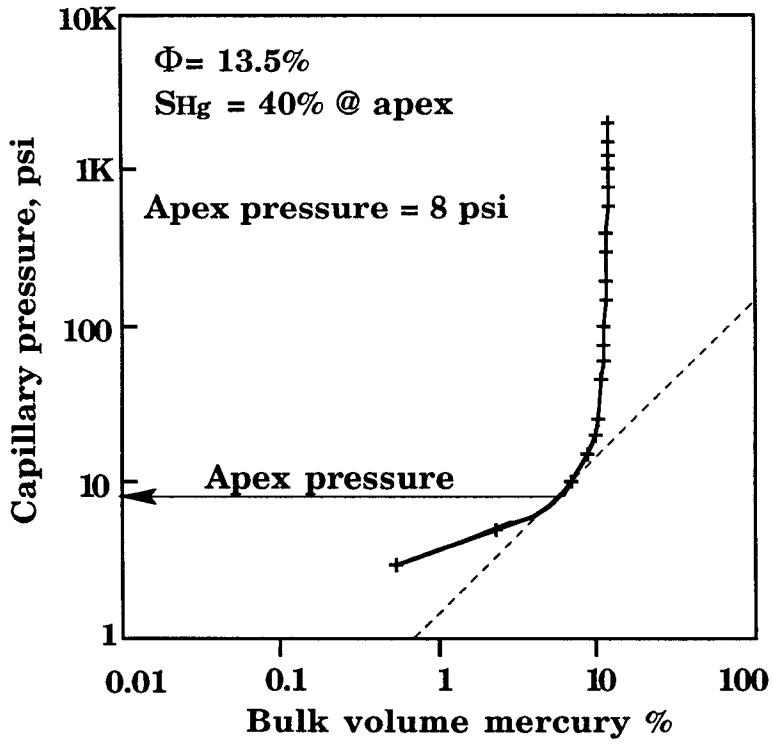

The entry pressure marks the lowest level at which hydrocarbons enter the rock. Numerous laboratory studies have been made to determine the pressure at which the non-wetting fluid of hydrocarbons would form a continuous well-connected network of filaments in the pores of the rock that dominated its fluid flow. Swanson (1977) determined that this point

corresponded to the apex of a hyperbola when the capillary pressure curve was plotted as a log-log plot of pressure against bulk volume of mercury. In the example shown, the *apex pressure* is about 8 psi at a bulk volume mercury of 5.4% and so, mercury saturation of 40% (because the porosity of the sample is 13.5%.

In addition to characterizing the key features of the capillary pressure curve, the pressure units can be converted into either (1) the radius of the pore throat that is entered by the non-wetting fluid or (2) the equivalent column of hydrocarbon that will provide the equivalent buoyancy pressure.

Remember that: $Pc = \frac{2\sigma\cos\theta}{r}$

Now, for the mercury/air system, $2\sigma\cos\theta = 107.6$. Therefore, $r = \frac{107.6}{Pc}$,

where r is the critical pore-throat radius entered at pressure, Pc, and measured in micron units (symbolized by μ and equivalent to one thousandth of a millimeter). A commonly used descriptive range scale of pore-throat sizes is:

Pore throat r, μ	Pore throat type	Entry pressure, psi
<0.1	NANO	1076
0.1 - 0.5	MICRO	215
0.5 - 2	MESO	54
2 - 10	MACRO	11
>10	MEGA	0

The buoyancy pressure necessary to provide these entry pressures is generated by the height of the hydrocarbon column and the difference between the hydrocarbon density and that of the formation water. The relationship is:

$$Pb = (\rho_w - \rho_{hc})gh$$

where Pb is the buoyancy pressure, ρ_W and ρ_{hc} are the densities of the formation water and hydrocarbon, g is the gravitational constant and h is the height above Free Water Level (FWL).

In order to relate capillary pressure with buoyancy pressure, the laboratory system of mercury/air must first be converted to a hydrocarbon/water system that is a match with the fluids in the reservoir to be modeled or analyzed. The basic conversion equation is: $Pc_R = Pc_L \cdot \frac{2\rho_R\cos\theta_R}{2\rho_L\cos\theta_L}$

where the ρs are the interfacial tensions and the θs are the contact angles of the two systems, reservoir (R) and laboratory (L). The conversion ratio can be expressed as a single value, C, so that: $Pc_R = C \cdot Pc_L$. Values for the reservoir fluid physical variables is still a matter of some speculation, although some of the major ideas are summarized in the following table.

CAPILLARY PRESSURE RELATIONSHIPS

CALCULATION of r, the radius of pore-throat in microns accessed at P_{cL} (lab-measured air/mercury) measured in psi :

$$r = \frac{2\sigma\cos\theta}{6.9P_{cL}} = \frac{107.6}{P_{cL}}$$

System	Contact angle, θ	Interfacial tension, σ
Air/mercury	140	485
Oil/water:	0 (or 30)	"25"(15-35)
Gas/water	0	"50" (30-70)

CONVERSION from P_{cL} (lab-measured air/mercury) to P_{cR} (reservoir hydrocarbon/brine) capillary pressure:

$$P_{cR} = P_{cL}\frac{2\sigma_R\cos\theta_R}{2\sigma_L\cos\theta_L} = P_{cL}.C$$

	(range)
Typical oil: C=0.067	(0.040-0.094)
Typical gas: C=0.135	(0.081-0.188)

ESTIMATION of h, height in feet above FWL (Free Water Level) from PcL in psi:

$$h = \frac{P_{cR}}{0.433\,(\rho_w - \rho_H)}$$

$$= \frac{P_{cL}.C}{0.433\,(\rho_w - \rho_H)}$$

Fluid	Density range
Gas	0.001 - 0.5
Oil	0.51 - 1.00
Brine	1.0 - 1.2

$$\rho_{oil} = \frac{141.5}{^{\circ}API + 131.5}$$

SENSITIVE VARIABLE:

There are a wide range of estimates reported for interfacial tension in the hydrocarbon/water systems under reservoir conditions. Vavra et al (1992) suggest the relation of oil/water tensions with API gravity as: <30 API, σ=30; 30-40 API, σ=21; >40 API, σ=15; and a contact angle of zero.

UNITS:

Capillary pressure, P_c in psi (pounds per square inch), interfacial tension in dynes/centimeter, contact angle in degrees, pore-throat radius in microns (μ-m or millionths of a meter), density (ρ) in grams per cubic centimeter.

Once C and/or Pc_R are established, then laboratory measurements of mercury/air capillary pressure can be converted into equivalent height of hydrocarbon column because:

$$h = \frac{Pc_R}{0.433(\rho_w - \rho_{hc})} = \frac{C \cdot Pc_L}{0.433(\rho_w - \rho_{hc})}$$

and solved for specific reservoirs.

Approximate relationships are used by many companies to convert lab measurements of mercury/air capillary pressure directly to the height of an equivalent column of an "average" oil or "average" gas, by inserting typical values for the fluid and gas physical variables and combining them into a single conversion constant. I suggest that the conversions:

$h_{OIL} = 0.7 \cdot Pc_{Hg}$ for oil and $h_{GAS} = 0.35 \cdot Pc_{Hg}$ for gas

are serviceable first order approximations for wildcat log analysis and are themselves "averages" of relationships that I have seen used by industry.

CAPILLARY PRESSURE CURVES OF SANDSTONES

The pore structure of sandstones is dominated by intergranular porosity of macro size, with variable amounts of microporosity contributed typically by chert and clay minerals, along with silt-size quartz. A dual porosity system is often the result, where distinct modes of pore-throat sizes can be recognized and attributed to elements that can be seen by the microscope and, especially, the scanning electron microscope (SEM).

A good example is provided by Swanson (1985) who shows and describes a capillary pressure curve from a sample of Paleocene sandstone. This sample has a porosity of 18% and the following three figures show the varieties of information that can be deduced from a laboratory record of pressure and mercury saturation.

In the first figure, the data is plotted on an arithmetic scale of pressure and saturation up to a pressure of 250 psi. Note the low displacement pressure that reflects the relatively large pore throats in the intergranular porosity. The curve is broadly asymptotic to a saturation of about 30% which can be used to estimate the "irreducible" water saturation, *Swi*. Recall that it has been suggested that *Swi* represents the fraction of water that is held by capillary forces within the micropores. Because a radius of 0.5 microns is often used in the literature as a pragmatic (but workable) boundary between macro pore-throats and micro pore-throats, a specific value for *Swi* can be read at this level which corresponds to a pressure of 215 psi in the mercury/air system. On the right-hand vertical axis of the figure, the mercury/air pressures of the left-hand vertical axis have been converted to equivalent heights of an "average" oil and "average" gas column that would generate the necessary buoyancy pressure to overcome the capillary forces. The conversion used the rule-of-thumb ratios of 0.7 (oil) and 0.35 (gas) described earlier.

In the second figure, the entire record of the laboratory measurements is graphed, this time on a semi-log plot. Notice that, in the limit, there is no "irreducible" saturation ; at a pressure of about 8000 psi the pore system is completely filled with mercury. This explains why some engineers dislike the term "irreducible". Of course, we would only observe saturations in this Paleocene sandstone reduced to true irreducible (zero) in oil columns of about 5600 feet (over a mile or close to two kilometers). In reality, more modest columns would occur and coincide with the broad range of pore-throat sizes that marks the overall hiatus between macro pores and micro pores in a granular system.

Finally, on the third figure, the Paleocene sandstone data is recast as a frequency polygon of the pore-throat sizes within the rock. The capillary pressure curve is actually a cumulative frequency plot of pore-throat sizes, so that the frequencies are generated easily by plotting differences in mercury saturation at successive increments of pressure. The frequency polygon shows three distinctive modes that reflect mega intergranular, meso kaolinite, and nano chert pore-throat groups as is verified by SEM pictures.

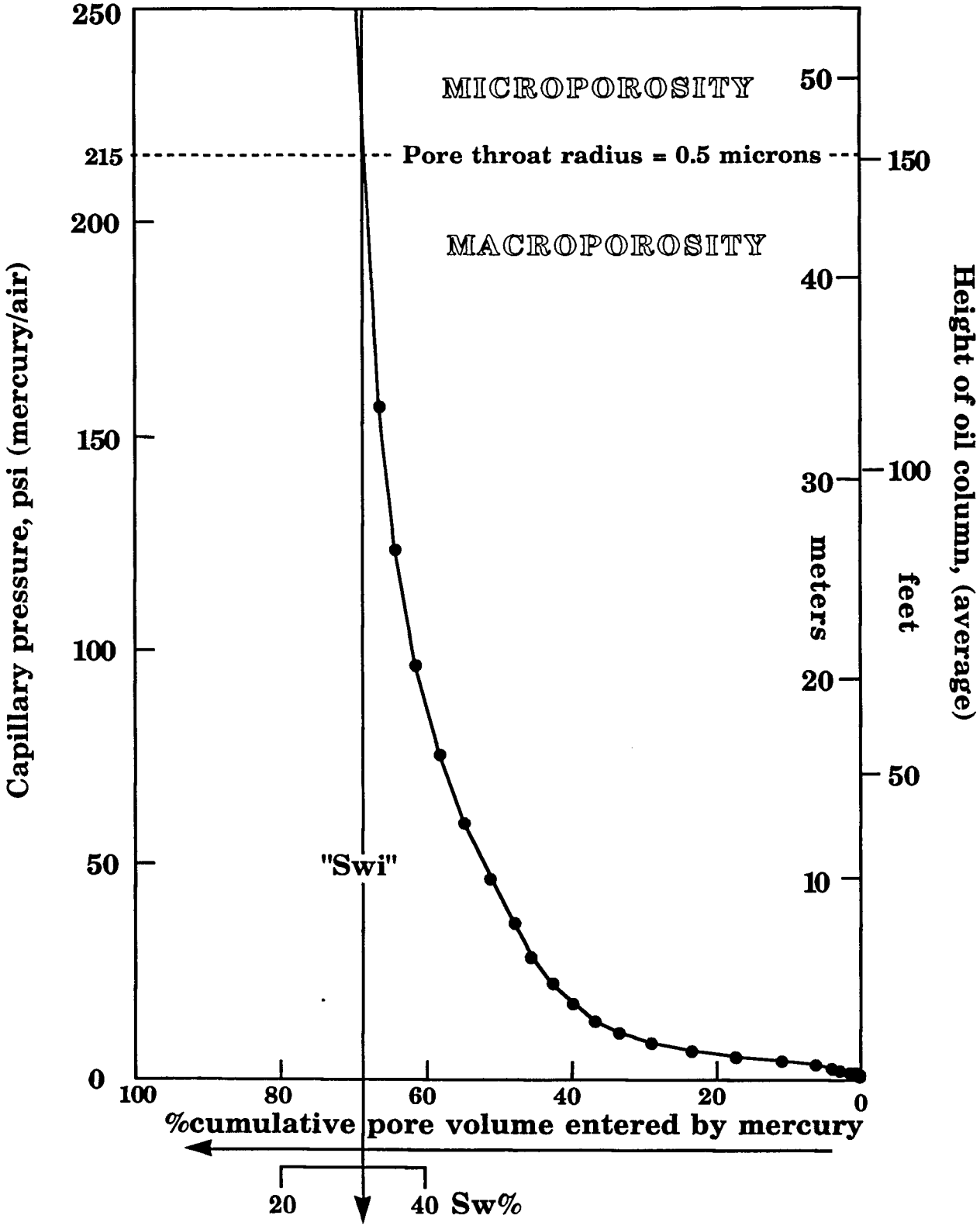

Cumulative volume of mercury injected into a Paleocene sandstone with a porosity of 18% (data from Swanson, 1985) plotted against capillary pressure and height of an equivalent column of typical oil.

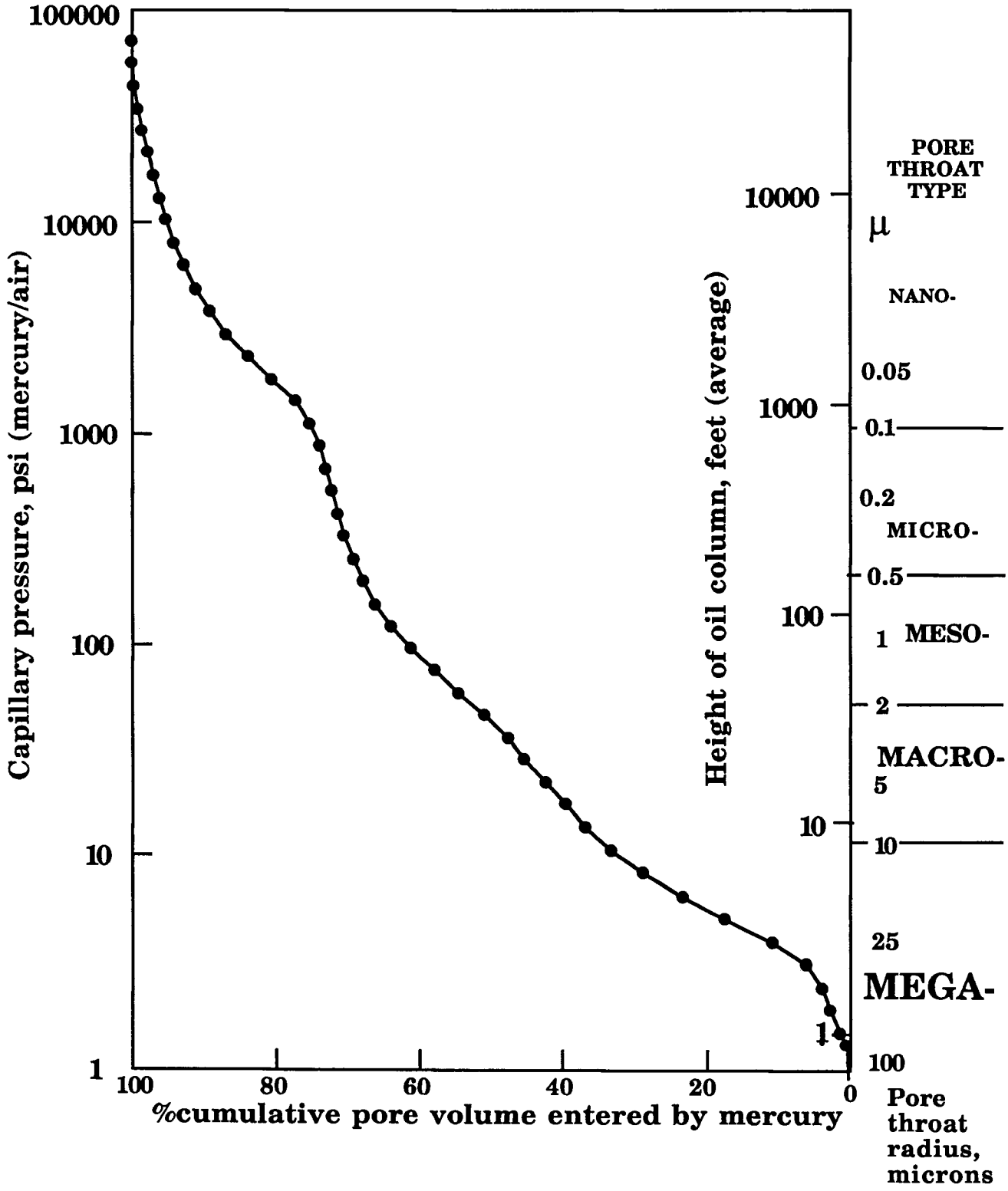

Cumulative volume of mercury injected into a Paleocene sandstone with a porosity of 18% (data from Swanson, 1985) plotted against capillary pressure, height of an equivalent column of typical oil, and equivalent pore-throat radius.

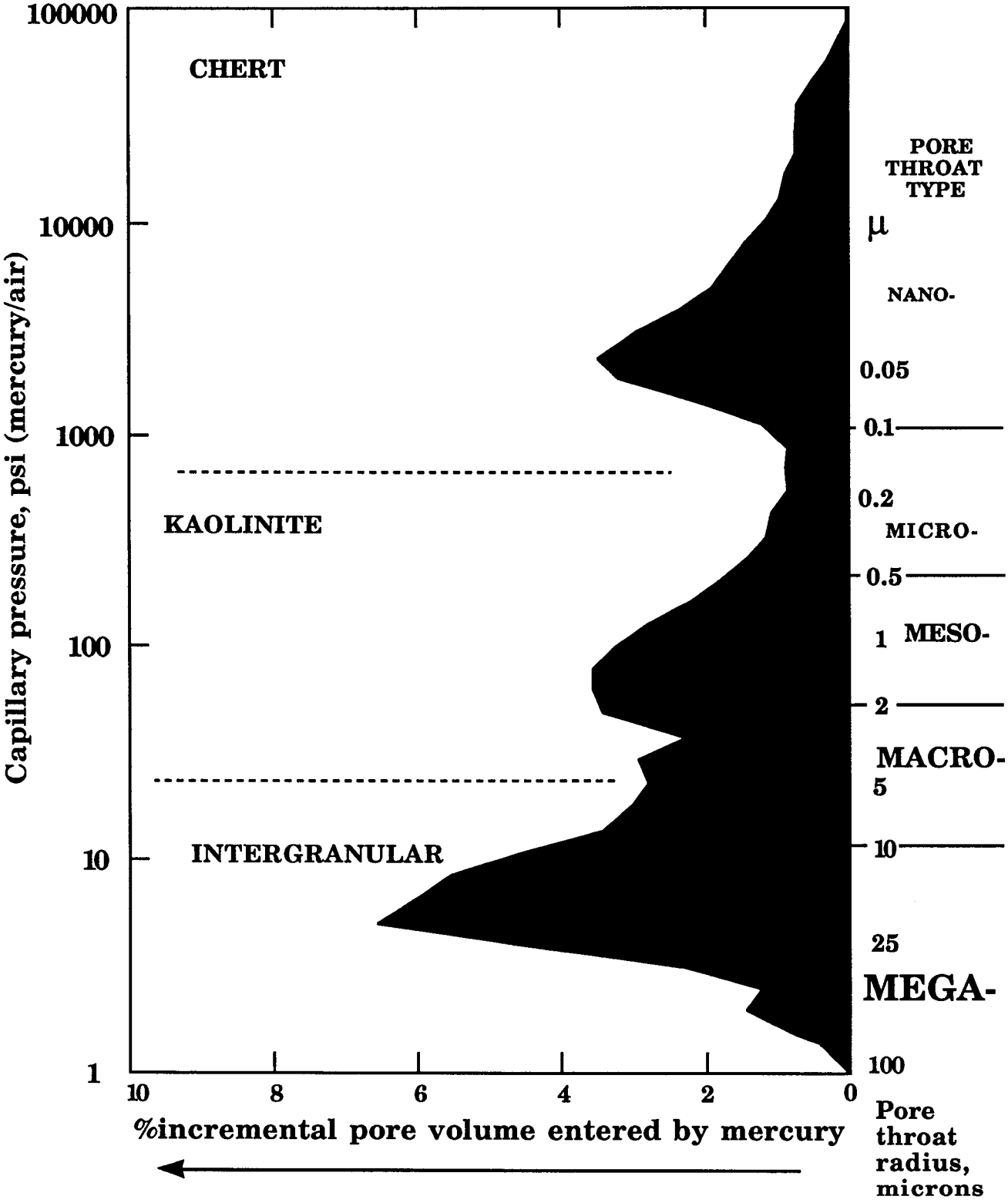

Incremental volume of mercury injected into a sandstone sample versus capillary pressure and equivalent pore-throat radius (data and SEM pictures from Swanson, 1985)

CAPILLARY PRESSURES OF CARBONATES

Not surprisingly, the capillary pressure curves of carbonates tend to be much more variable in character than sandstones, because of the great variety of pore sizes and shapes than can occur. However, many carbonate reservoirs are either relatively homogeneous (for petrophysical analysis purposes) or can be subdivided between a few distinctive petrofacies. Markedly heterogeneous heterogeneous carbonate reservoirs require more work, but it is in precisely these cases that capillary pressure measurements can provide both the numerical and conceptual keys to making sense of what otherwise would be mysterious log responses.

The illustration shows a panel of different pore/pore-throat types and their capillary pressure curves and pore-throat frequencies described by Luo and Machel (1995) in the Devonian Grosmont Formation of western Canada. The giant heterogeneous reservoir produces heavy oil from rocks that are dolomitized and karstified platform and ramp carbonates.

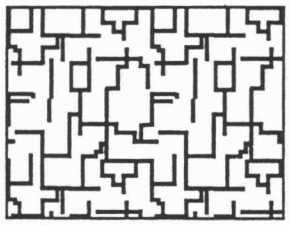

Pervasive solution -enlarged porosity; homogeneous pore throat and porosity; small pore-to-throat size ratio

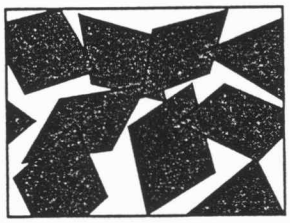

Dolomite rhombs; good crystal sorting; mainly intercrystalline porosity

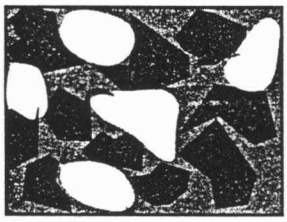

Heterogeneous texture of oversized pores, tight matrix blocks, and intercrystalline pores

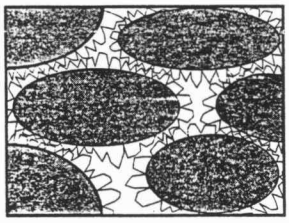

Dual-porosity texture of intergranular/ intercrystalline microporosity and ig/ix mesoporosity

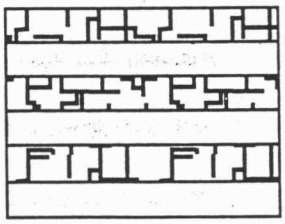

Pore throat textures consist of alternating laminations of two sizes of pores

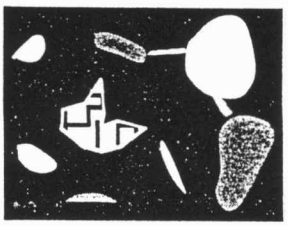

Heterogeneous, but non-random texture of tight matrix with variably sized pores and isolated vugs.

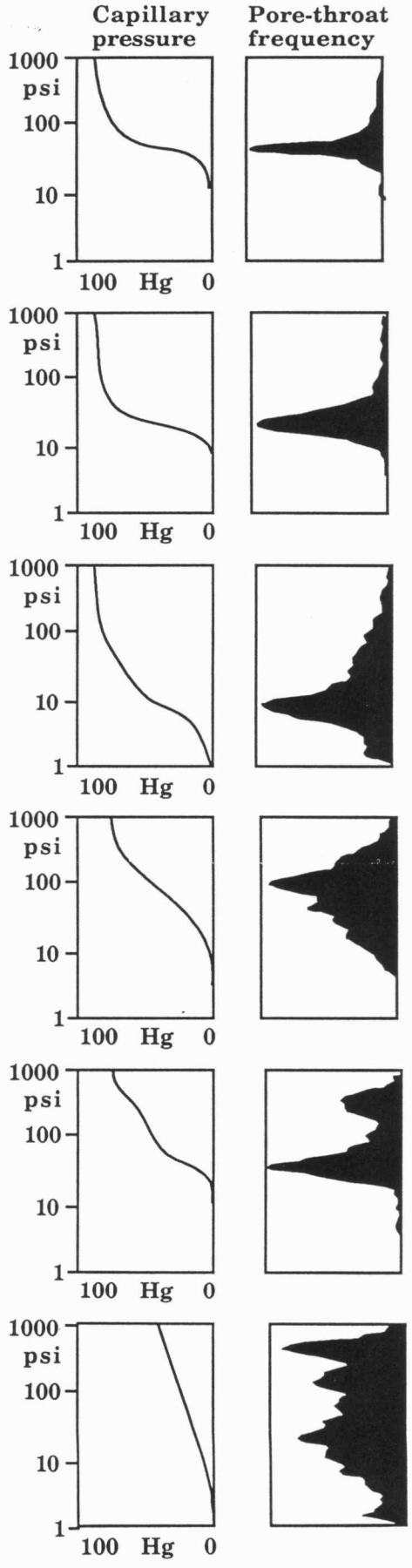

Carbonate reservoir heterogenity: Categories of pore-throat textures and their capillary curves in the Grosmont Formation (Devonian, Western Canada). Adapted from Luo and Machel (1995).

INTEGRATION OF CAPILLARY PRESSURE MEASUREMENTS WITH LOG ANALYSIS: AN EXAMPLE

Core plug samples were taken from a Mississippian oil field in south-west Kansas which produces oil from a few thin and isolated reservoir intervals. The field trap is a stratigraphic pinchout with some additional structure that has about 50 feet of closure. However, the maximum observed oil column of the reservoir intervals is less than 20 feet. The reservoir facies is made up of subtidal ooid-skeletal grainstones with well-preserved interparticle porosity. Downdip, the interparticle porosity in this subtidal lithofacies has been partially occluded by cementation and becomes a marginal reservoir facies. The updip seal facies appears to be shaly shelf to shaly tidal flat deposits.

Capillary pressure data from plugs that are representative of these three reservoir lithofacies are listed in the table. Pressures have been converted to equivalent pore-throat radii and estimated height of oil column. Rather than use the rule-of-thumb pressure/oil height conversion ratio of 0.7, a custom tailored ratio was developed using the physical properties listed at the foot of the table. In this instance, the ratio was computed to be 0.703, a fortuitous match with the rule-of-thumb number and a coincidence that should not be relied on to occur in other detailed field studies.

Overleaf, the capillary pressure data for the good reservoir rock (sample #3) are plotted against mercury saturation together with a schematic that shows the method to construct a frequency histogram of pore-throat sizes from these capillary pressure data. Notice how this reservoir facies is dominated by mega-size pore throats. Capillary pressure data are also plotted for all three samples on a graphic chart (a "blank" of this plot can be found in Charts). The chart axes are scaled in pressure, pore-throat radius, and heights of equivalent columns of "average" oil and "average" gas. The marked differences between these three lithofacies are immediately apparent and the plot can be used for traditional capillary pressure interpretations such as the maximum hydrocarbon column that could be sustained by the seal facies before it was breached, or the minimum closure that would be needed for a trap before water-free oil could be produced.

In this course, we consider how the capillary pressure data can be integrated directly into the log analysis methods that we have used up to this point.

Capillary pressure data of the St. Louis Limestone (Mississipian) from southwest Kansas.

Sample #1 = Updip **seal** of shaly shelf to shaly tidal flat deposits ;
Sample #2 = Downdip **marginal reservoir** subtidal lithofacies with interparticle porosity partially occluded by cement ;
Sample #3 = **Good reservoir** subtidal ooid-skeletal grainstones with well-preserved interparticle porosity.

Pc psi	r μ	h feet	#1 Sm%	#2 Sm%	#3 Sm%
1.0	108	0.7	0.0	3.3	0.8
2.0	54	1.4	0.0	5.0	2.1
3.0	35.9	2.1	0.0	5.7	3.9
5.0	21.5	3.5	0.0	7.1	17.0
10.0	10.8	7.0	2.2	12.1	51.1
15.0	7.2	10.5	3.5	19.4	65.1
20.0	5.4	14.1	3.5	25.1	71.4
25.0	4.3	17.6	3.5	32.2	74.7
45.0	2.4	31.6	3.5	50.5	79.6
60.0	1.8	42.2	3.5	56.0	81.1
75.0	1.4	52.7	3.5	59.3	81.9
100.0	1.1	70.3	3.5	62.4	82.9
150.0	0.72	105.5	3.5	65.8	84.1
200.0	0.54	140.6	3.5	67.5	84.7
300.0	0.36	210.9	5.2	70.0	85.6
400.0	0.27	281.2	5.8	72.2	86.2
600.0	0.18	421.8	6.9	77.0	86.9
800.0	0.13	562.4	7.5	82.5	87.6
1000.0	0.11	703.3	7.5	87.0	88.0
1200.0	0.09	844.0	8.7	90.5	88.5
1500.0	0.07	1055.0	8.7	93.6	89.1
2000.0	0.05	1406.6	14.5	97.2	89.9
		Porosity%	1.3	9.3	13.5
		Permeability,md	<0.1	5.0	311

Pc= capillary injection pressure, mercury-air, psi
Sm%= pore percentage saturation of mercury

r= pore throat radius in microns, estimated from r= 107.6/Pc
h estimated using following field data: Oil gravity = 43 API; oil density= 0.81 gm/cc.; brine density= 1.03 gm/cc.; and parameters: Air/mercury contact angle of 140 degrees and interfacial tension of 485 dynes/cm; oil/water contact angle of 0 degrees and interfacial tension of 25 dynes/cm. Relationship is then: h= 0.703 PcL.

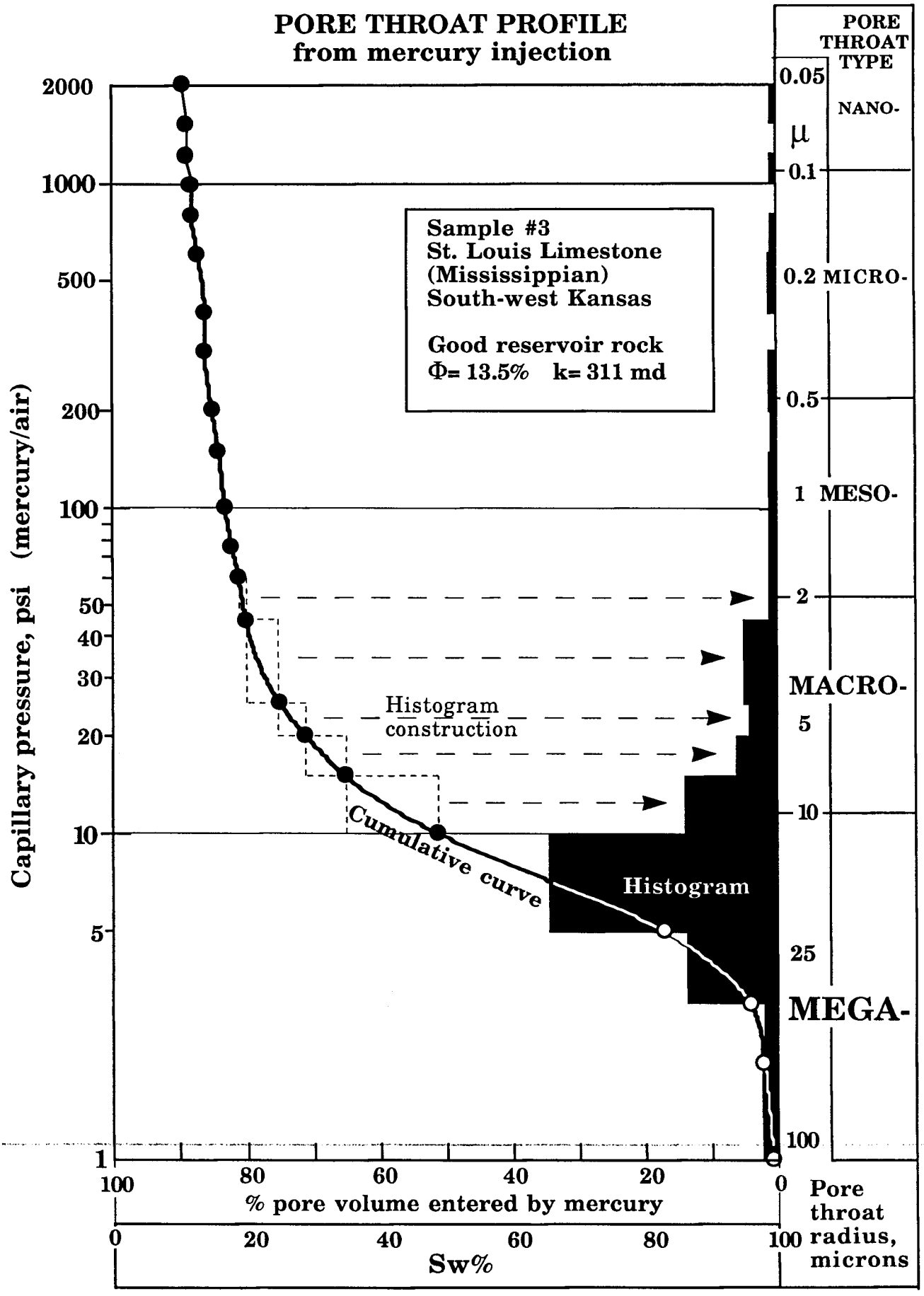
PORE THROAT PROFILE
from mercury injection
PORE THROAT TYPE
Sample #3
St. Louis Limestone
(Mississippian)
South-west Kansas
Good reservoir rock
Φ= 13.5% k= 311 md
Capillary pressure, psi (mercury/air)
2000
1000
500
200
100
50
40
30
20
10
5
1
0.05
μ
0.1
0.2
0.5
1
2
5
10
25
100
NANO-
MICRO-
MESO-
MACRO-
MEGA-
Histogram construction
Cumulative curve
Histogram
100 80 60 40 20 0
% pore volume entered by mercury
0 20 40 60 80 100
Sw%
Pore throat radius, microns

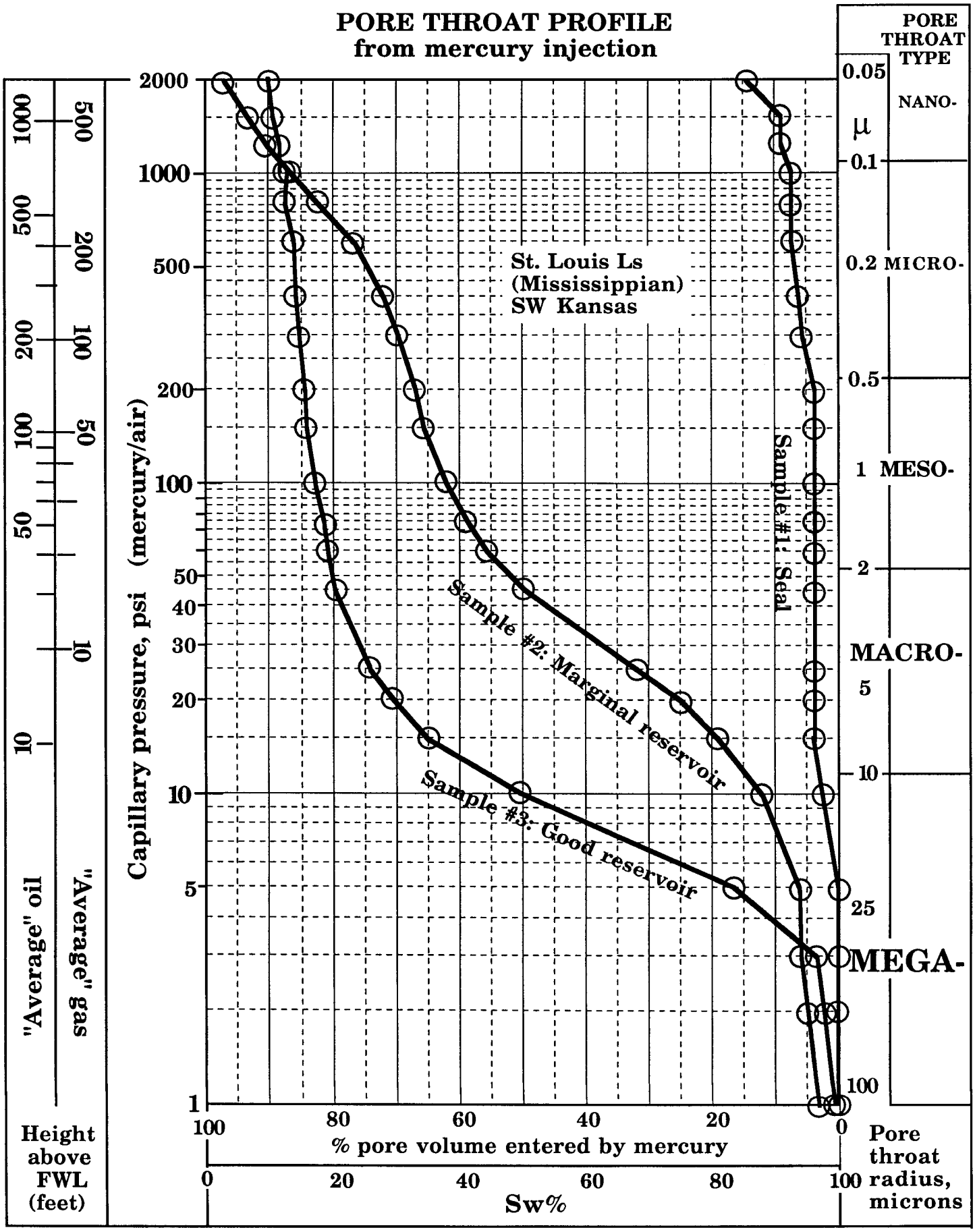
PORE THROAT PROFILE
from mercury injection
PORE THROAT TYPE
NANO-
MICRO-
MESO-
MACRO-
MEGA-
0.05
μ
0.1
0.2
0.5
1
2
5
10
25
100
St. Louis Ls
(Mississippian)
SW Kansas
Sample #1: Seal
Sample #2: Marginal reservoir
Sample #3: Good reservoir
Capillary pressure, psi (mercury/air)
2000
1000
500
200
100
50
40
30
20
10
5
1
"Average" oil
"Average" gas
1000
500
200
100
50
10
Height above FWL (feet)
100
80
60
40
20
0
% pore volume entered by mercury
0
20
40
60
80
100
Sw%
Pore throat radius, microns

In the schematic figure on the next page, capillary curves are shown for three hypothetical samples which range from low porosity (and permeability), Φ_1, to high porosity (and permeability), Φ_3. Diagrams of this kind are not uncommon in the petroleum engineering literature, where representative curves are shown for a specific reservoir and the curves are either "typical" examples or some kind of generalized average. If a reservoir is moderately homogeneous in a petrofacies sense, the curves serve as reference features for a continuum, so that curves for intermediate porosities can be deduced by interpolating between the plotted curves. The capillary pressure curves are therefore contours of the mapping of porosity into a reference space of capillary pressure and mercury saturation.

Although the laboratory measurements record mercury saturation, the remaining pore space is equivalent to water saturation as would be observed in the reservoir. The mapping is therefore a representation of porosity in capillary pressure - water saturation space. Now, the Buckles plot is itself a mapping system , with axes of porosity and water saturation. As shown by the diagram, it is possible to remap from one system to the other: from porosity in pressure-water saturation space to pressure in porosity-water saturation space. Each curve translates to a sequence of pressure points located along a porosity isoline that matches the porosity of the curve sample, and with positions at their corresponding water saturation. We could imagine that pressure was now a vertical axis projecting upwards and that we were looking down on the curves, with the pressure points showing the elevation of the curves above the surface of the plot.

In the next step, we link common pressure points by lines to form pressure contours on the Buckles plot. This interpolation process is equivalent to interpolating additional pressure curves between the three original reference curves. In either case, the interpolation is only valid if the interpolated curves or contours would be a reasonable match with actual pressure data for a core sample with the interpolated porosity. In other words, the processed curves are considered to represent a single petrofacies. If they are not, then separate mappings should be developed from subsets of curves that constitute distinct petrofacies. The process will be the same, only executed as a stratified approach to the reservoir with subdivision between separate petrofacies, rather than a representation by a single petrofacies.

The Buckles plot projection will itself give useful signs as to whether curves selected for interpolation constitute a single petrofacies. Notice that the pressure levels Cp_1, Cp_2, and Cp_3 are equally spaced on the capillary pressure plot. However, their mapped contours show an asymptotic convergence on a hyperbola on the Buckles plot. This hyperbola is an expectation that would be matched by the trends observed empirically by Buckles in his work with Canadian reservoirs. As suggested earlier, the Buckles number can be considered to represent the proportion of microporosity in the rock. This concept

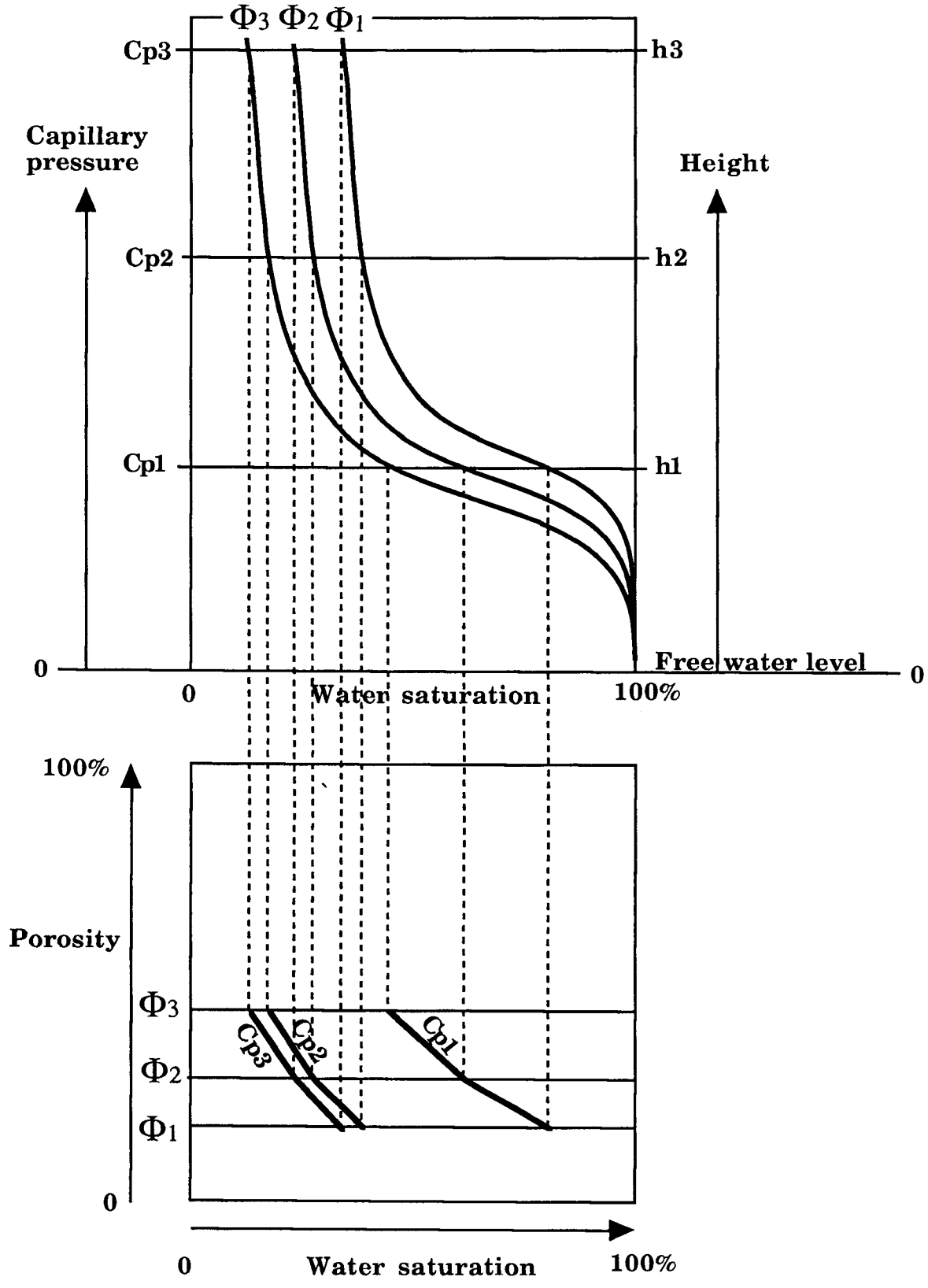

Mapping capillary pressures (or height of hydrocarbon column) to a porosity- water saturation crossplot.

is certainly consistent with their equivalent position on the pressure axis of the capillary pressure curve plot at levels at the macro/micro pore throat boundary.

If the projected contours show strange or erratic patterns, the aberrations can themselves be used to subdivide the pressure curve sets into separate petrofacies subsets keyed to different Buckles numbers.

Notice that heights of equivalent oil or gas column may be substituted for capillary pressure. This alternative scaling will be particularly useful on the Pickett plot, so that comparisons can be made easily between column height and stratigraphic depths of zones marked on the plot.

In this Mississippian example, it is reasonable to propose that the tidal flat lithofacies as a single petrofacies ranging from porous updip reservoir to less porous, cement-occluded downdip marginal reservoir. Pressure data from samples #2 and #3 are projected onto the Buckles plot and linked by contours that represent predictions of pressure and saturations at intermediate porosities. The contours are marked both with their capillary pressure values and the equivalent height of oil column in feet. The trends conform approximately with the expectation for a simple Buckles model (constant *c*) and so, interpolation appears to be a justifiable procedure.

The Buckles plot suggests a Buckles number (*c*) of about 0.03 for this Mississippian reservoir. This "irreducible" saturation state appears to be reached by a column of about 50 feet of oil. In a good reservoir facies with 13.5% porosity this would mean an expected "irreducible" water saturation, *Swi* of about 22%. Recall that the critical water saturation, *Swcrit*, (the highest water saturation at which water-free production will occur) is generally a little higher than *Swi*, based on core studies of relative permeability. Since we have no core data on relative permeabilities, we could use the rule-of-thumb estimate of:

$$Sw_{crit} = \sqrt{Sw_i}$$

which would result in a value of 47%. The number seems a little high for this facies, but we will bear it in mind as we proceed with a Pickett plot presentation of capillary pressure data and their reconciliation with log data from a Mississippian section in the field.

BUCKLES PLOT

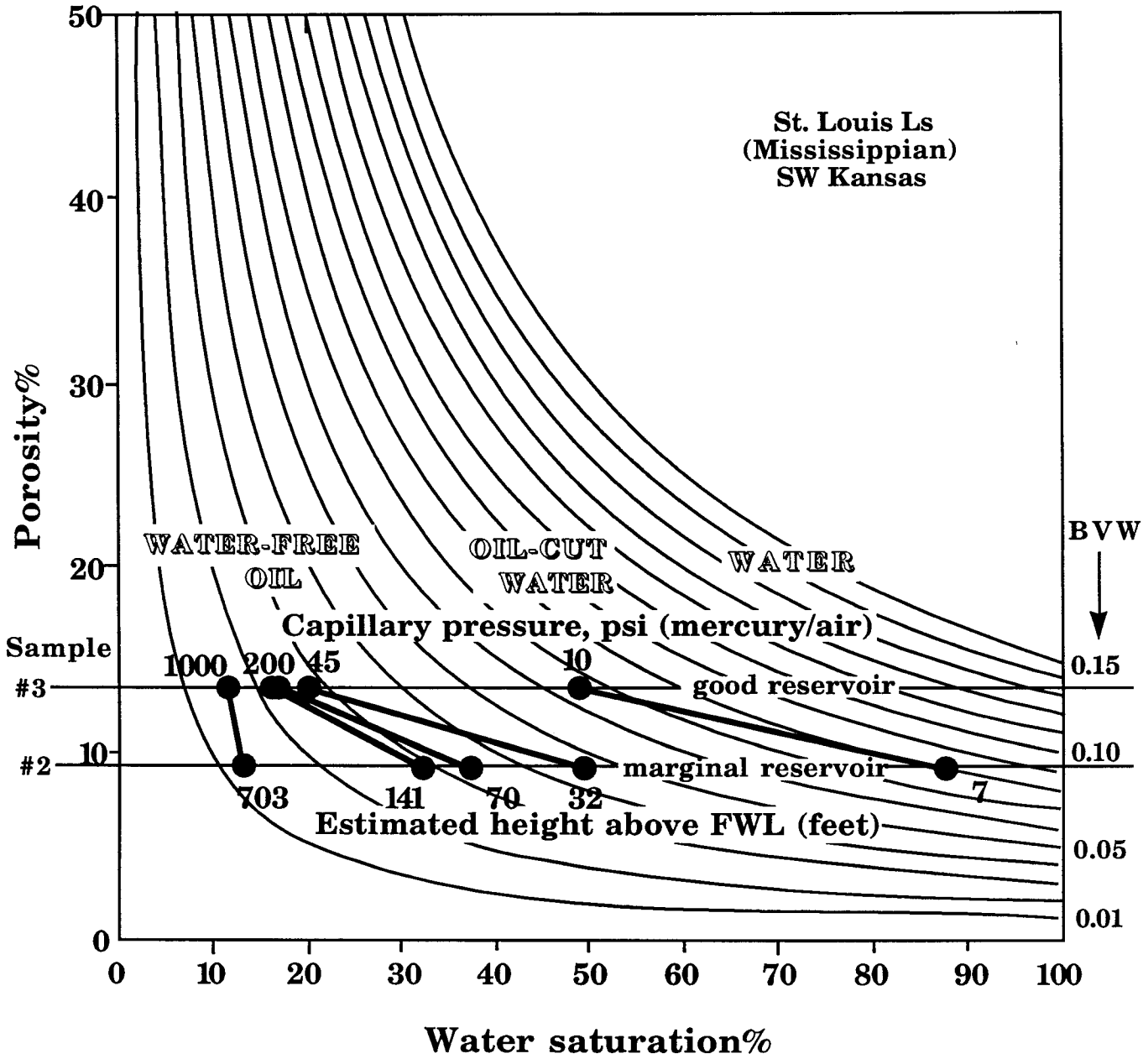

The Buckles plot and the Pickett plot are alternative mappings that we can use for capillary pressure data. The fundamental porosity and water saturation axes are present on both : as orthogonal axes on the Buckles plot; oblique axes on the Pickett plot. The schematic figure shows pressure data from the three hypothetical capillary pressure curves plotted on both kinds of plot. The choice of Pickett plot can be conventional (as shown) with resistivity-porosity axes and an intercept of water resistivity, *Rw*, at the 100% porosity level. Alternatively the "standardized" Pickett plot with axes of the resistivity ratio *Rt/Rw* and porosity may be used. A major advantage of the standardized version is that variation in water resistivity is no longer an issue, so that the same plot can be used across a field or even an entire basin, provided that the capillary pressure data remains representative of the formation rock type.

As with the Buckles plot presentation, contours may be made of either capillary pressure itself, or of equivalent height of hydrocarbon column. Logging data of resistivity and porosity measurements from the subsurface formation zones can now be plotted and related directly to capillary pressure data. The interpretations are basically an extension of the pattern recognition concepts used earlier, where the data were used to draw conclusions using a *conceptual* model of reservoir structure and the empirical model of Buckles. Now the data are related to an *explicit* model where contours are controlled by physical measurements from core. As discussed before, the interpolated contours depend on the assumption of common petrofacies association, so that petrofacies recognition and distinction are an integral part of the analysis procedure. In the conclusion of the SW Kansas Mississippian example, we shall see how this assumption can be checked in the reconciliation phase that matches log data with capillary pressure data. If necessary, it may be necessary to modify the model to obtain a better reconciliation.

Capillary pressure contours tagged with both their pressure values and equivalent oil column heights are drawn on a standardized Pickett plot. Archie equation constants of a=1 and m=1.8 were used to draw the water line with an intercept of a *Rt/Rw* ratio value of unity at 100% porosity. The comparatively low value of m had been found previously to be a better choice than m=2, and was explained by the granular texture of porosity in this facies. Once the water line is established, water saturation lines can be generated using exactly the same techniques as described earlier.

On the following page, logs are shown from a Mississippian section in a typical producing well in this SW Kansas field. Porosity and resistivity readings were taken from the logs at one-foot intervals and plotted on a standardized Pickett plot. The log data pattern suggests a total oil column of about 16 feet which would be an excellent match with a number predicted from field engineering data. Although the upper few feet of the porous reservoir are represented well, the lower, less porous section appears to be at variance with the interpolated contours. Eight feet of the section occur in what was predicted

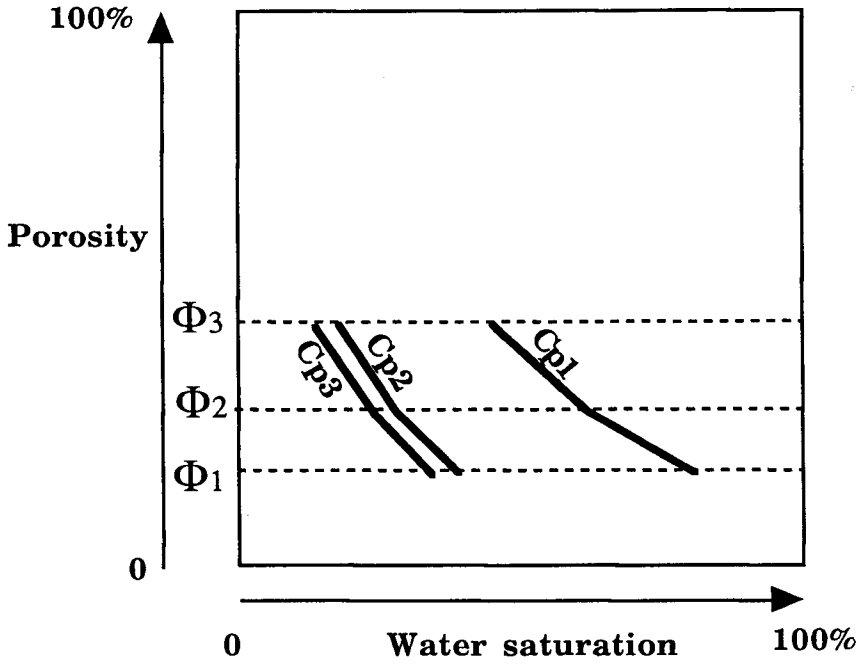

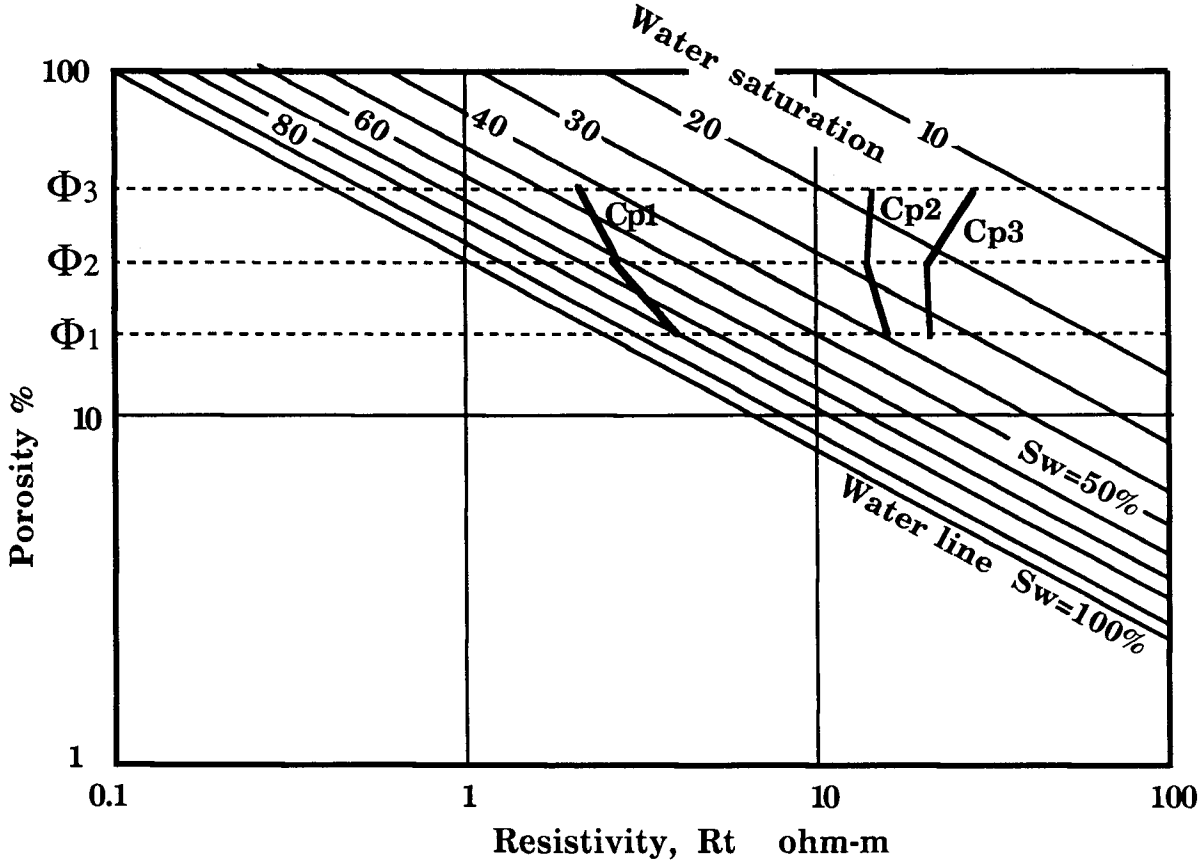

Alternative mappings of capillary pressure in porosity-water saturation space: graphed on orthogonal axes (above); and on oblique axes on the Pickett plot (below).

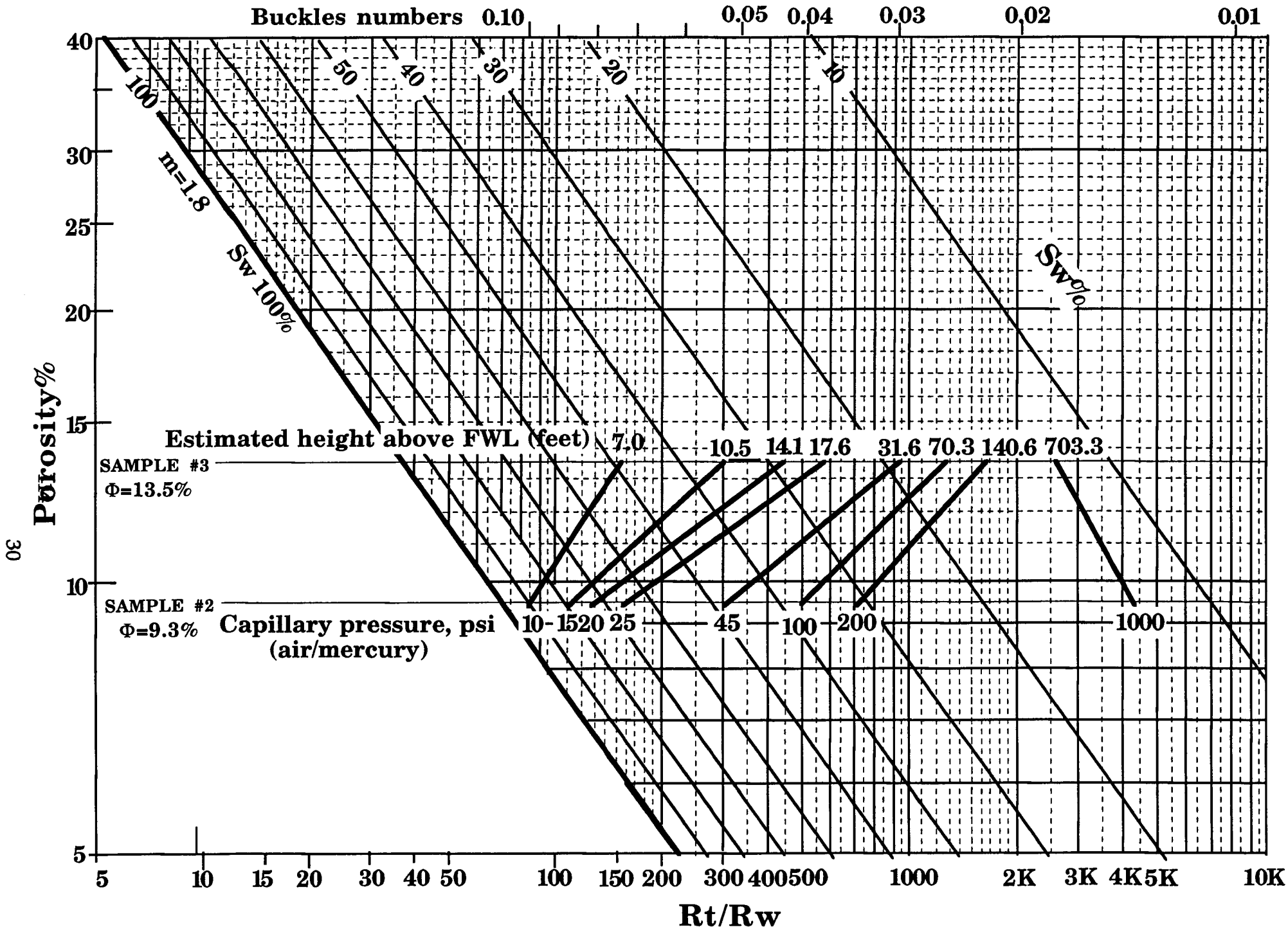
Buckles numbers 0.10 0.05 0.04 0.03 0.02 0.01
100
50
40
30
20
10
m=1.8
Sw 100%
Sw%
Porosity%
Estimated height above FWL (feet)
7.0
10.5
14.1
17.6
31.6
70.3
140.6
703.3
SAMPLE #3
Φ=13.5%
SAMPLE #2
Φ=9.3%
Capillary pressure, psi
(air/mercury)
10
15
20
25
45
100
200
1000
40
30
25
20
15
10
5
5
10
15
20
30
40
50
100
150
200
300
400
500
1000
2K
3K
4K
5K
10K
Rt/Rw

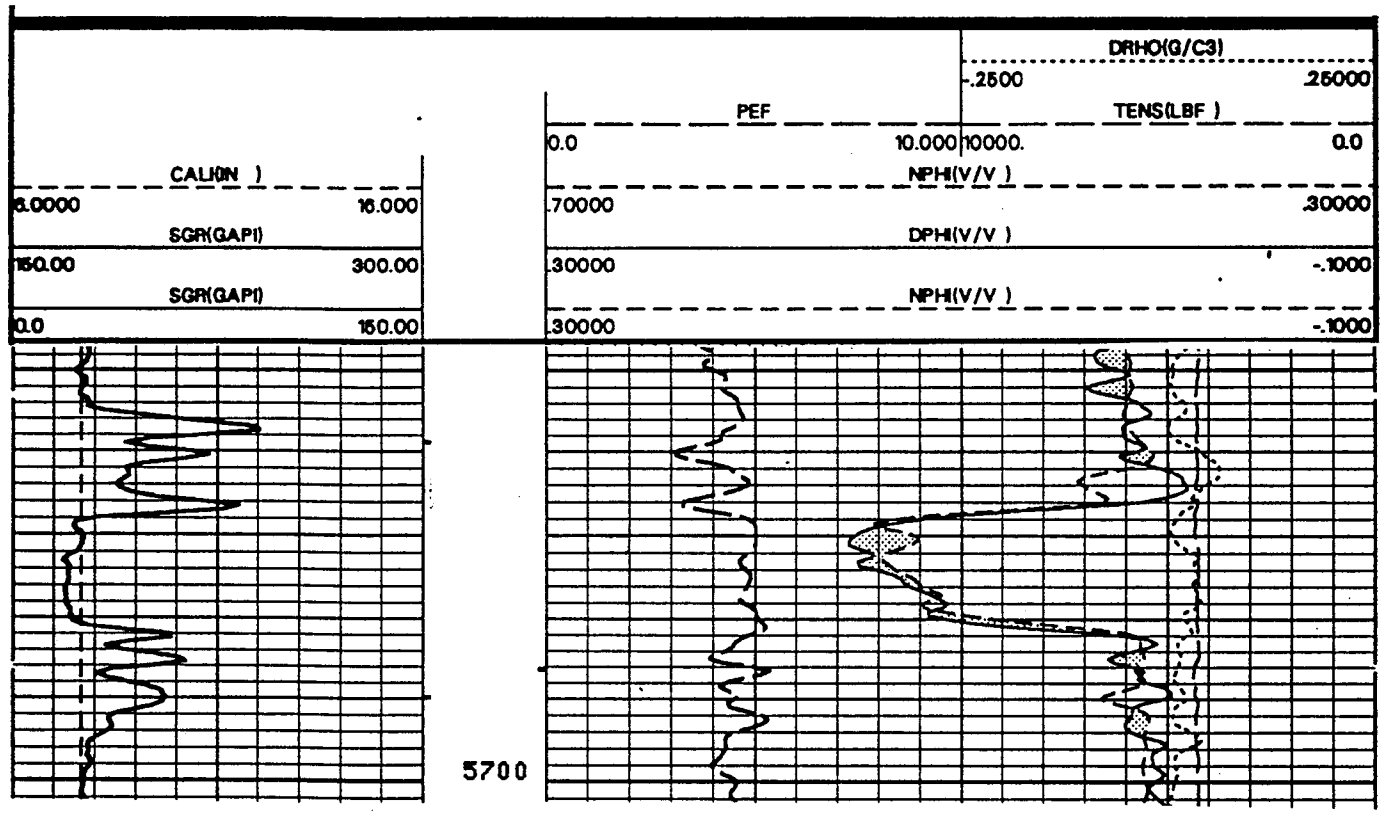

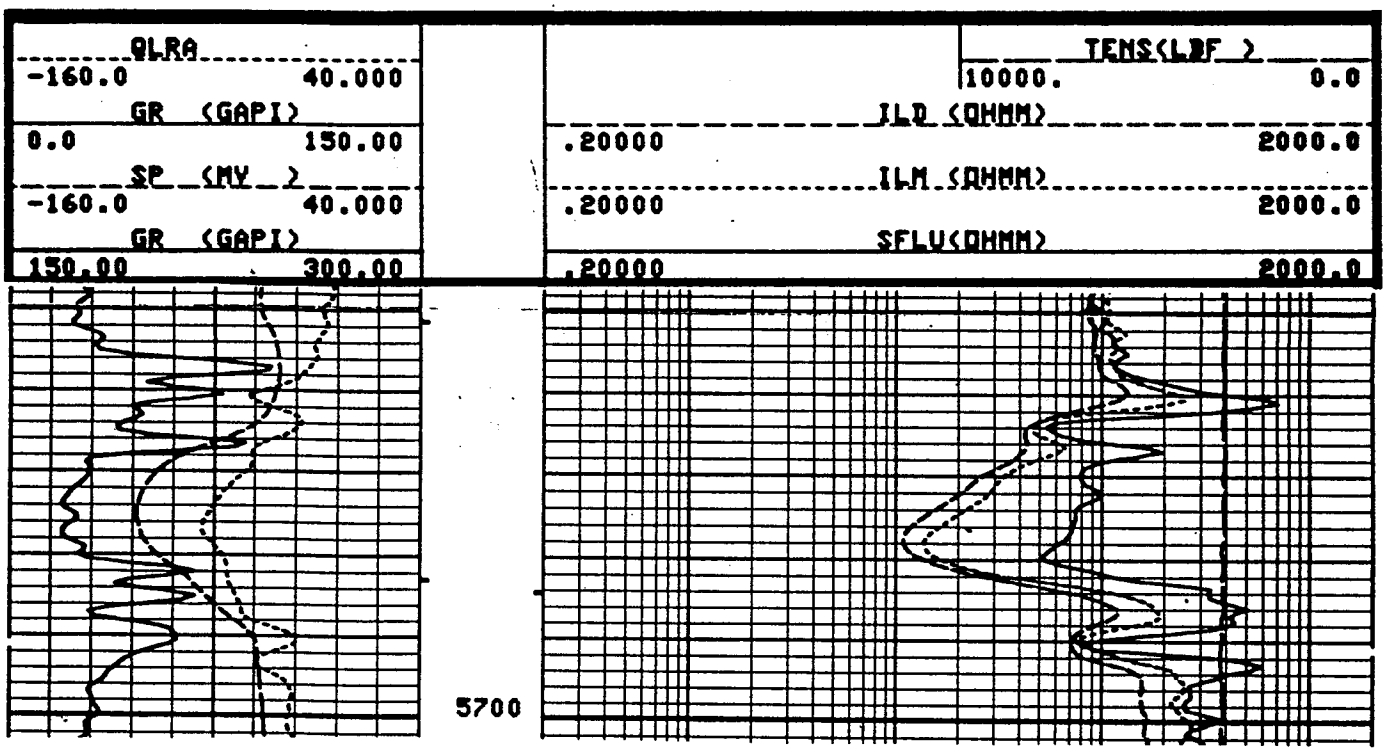

Mississippian well, SW Kansas:
Analysed interval: 5667 - 5681 feet sub-KB
Perforated interval: 5666 - 5672
IPP: 240 BO, 70 BWPD

to be only two feet of oil column. It is probable that this lower section is poorly represented by values extrapolated to down-dip cemented marginal reservoir facies. It appears that the two lithofacies are represented by two separate petrofacies that may be laterally adjacent, but not vertically contiguous. In a modified model, sample #1 could be retained as good reservoir petrofacies data and, in the absence of other plug measurements, the pressure points extrapolated parallel to the Buckles number contours. The modification would provide an improved fit between log data and capillary pressure contours. If valid, the extrapolation implies that the petrofacies has a common value for microporosity regardless of total porosity across its range in the spirit of the Buckles model.

A modified Pickett plot is shown where the contours of height above FWL are sketched using (i) a total oil column of 16 feet and (ii) the depth increment of one foot between log data points. The height contours can then be mapped back onto a capillary pressure plot. In the example shown, two hypothetical capillary pressure curves are plotted, one for 10%, the other for 20% porosity, based on the modified Pickett plot. The ability to BOTH map measured capillary pressure data onto a Pickett plot AND to reverse the process in mapping logged data from a Pickett plot on to a capillary pressure plot is valuable in reconciling laboratory and field data in a single procedure. Of course, it some instances, there will be inconsistencies or discrepancies between the two sources of data, but these conflicts will become readily apparent.

Ultimately, it must be recognized that logging tool errors of all kinds, vertical resolution problems, and the inadequacy of a few plugs to represent complex reservoirs will mean that an excellent match can only be *expected* in simple, homogeneous reservoirs. However, the discussion outlined in this example has tried to demonstrate that the best strategy may involve working hypotheses, modifications of models, pattern recognition, and data reconciliation in the grand traditions of classic log analysis.

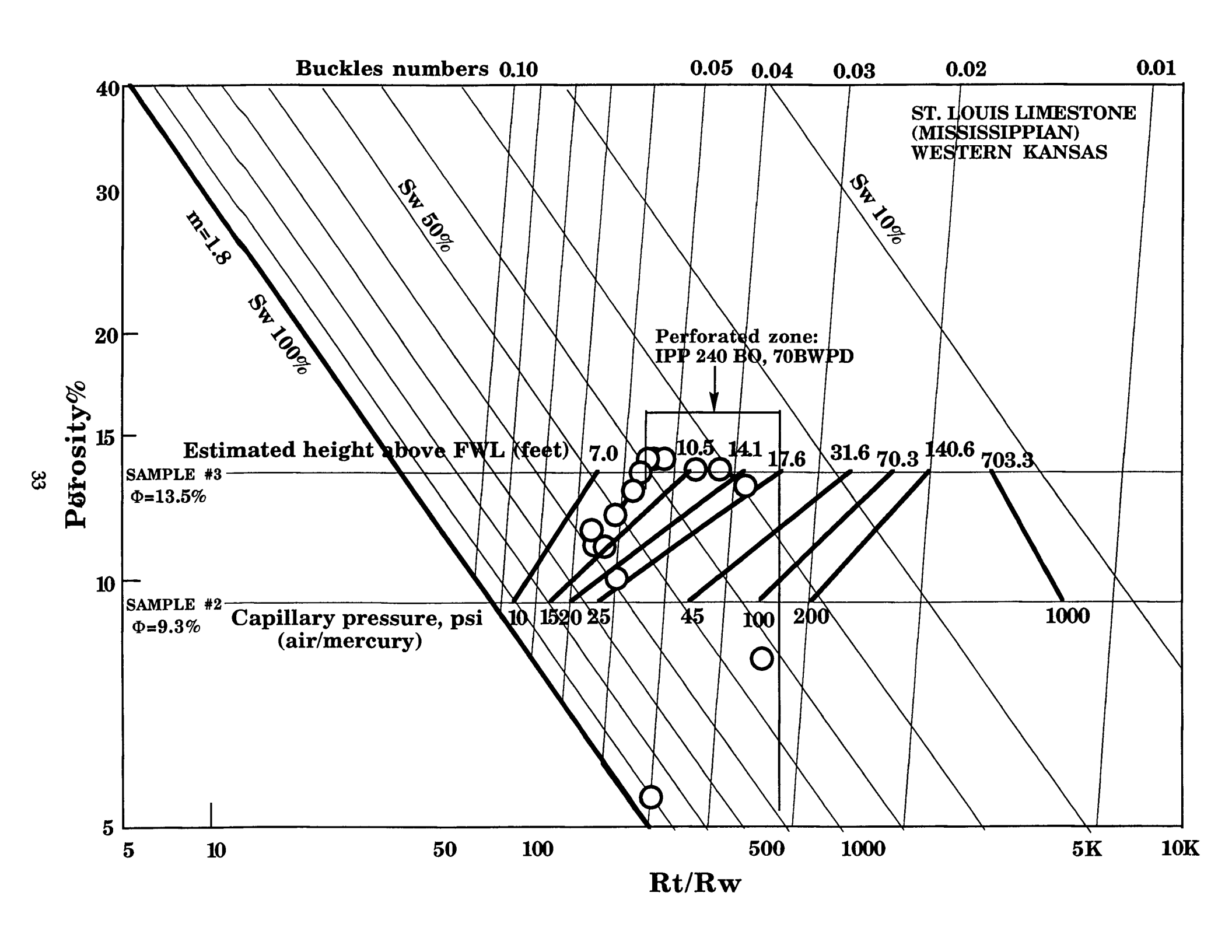
Buckles numbers 0.10
0.05
0.04
0.03
0.02
0.01
ST. LOUIS LIMESTONE
(MISSISSIPPIAN)
WESTERN KANSAS
m=1.8
Sw 100%
Sw 50%
Sw 10%
Perforated zone:
IPP 240 BO, 70BWPD
Estimated height above FWL (feet)
7.0
10.5
14.1
17.6
31.6
70.3
140.6
703.3
SAMPLE #3
Φ=13.5%
SAMPLE #2
Φ=9.3%
Capillary pressure, psi
(air/mercury)
10
15
20
25
45
100
200
1000
Porosity%
40
30
20
15
10
5
5
10
50
100
500
1000
5K
10K
Rt/Rw

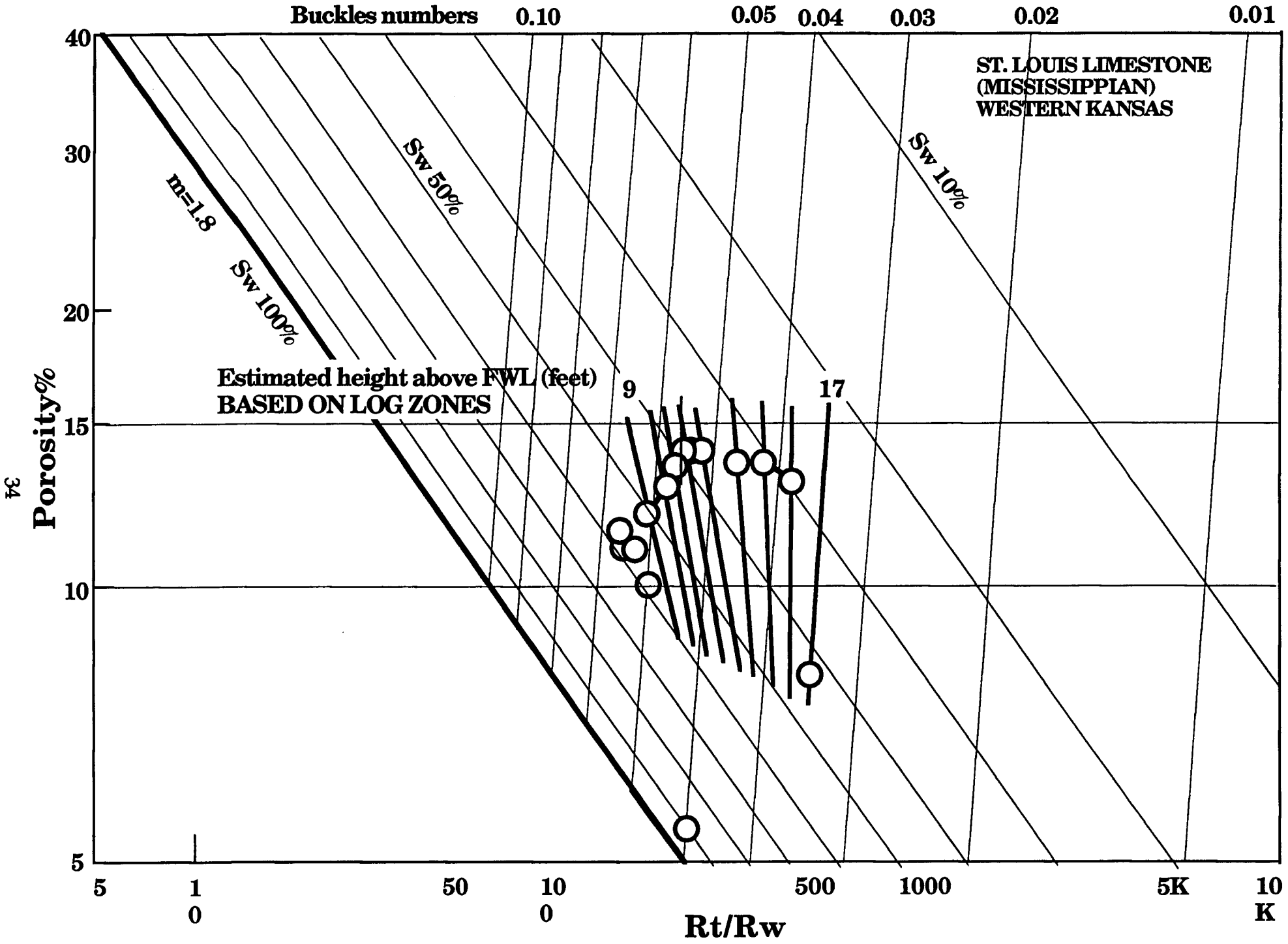
Buckles numbers
0.10
0.05
0.04
0.03
0.02
0.01
ST. LOUIS LIMESTONE
(MISSISSIPPIAN)
WESTERN KANSAS
Sw 50%
Sw 10%
m=1.8
Sw 100%
Estimated height above FWL (feet)
BASED ON LOG ZONES
9
17
Porosity%
40
30
20
15
10
5
5
1
0
50
10
0
500
1000
5K
10
K
Rt/Rw

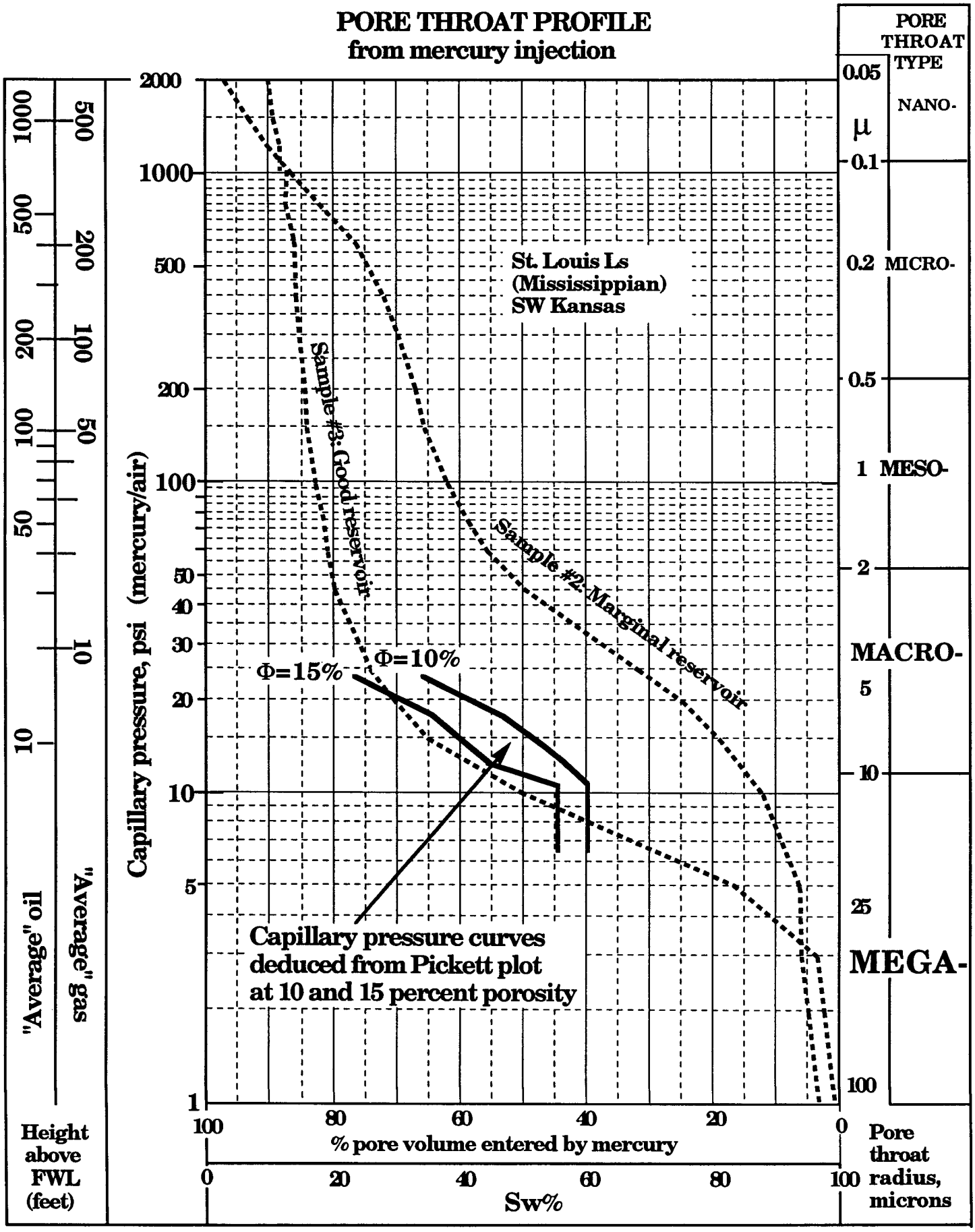
PORE THROAT PROFILE
from mercury injection
PORE THROAT TYPE
0.05
NANO-
μ
0.1
0.2 MICRO-
0.5
1 MESO-
2
MACRO-
5
10
25
MEGA-
100
St. Louis Ls
(Mississippian)
SW Kansas
Sample #3: Good reservoir
Sample #2: Marginal reservoir
Φ=15%
Φ=10%
Capillary pressure curves
deduced from Pickett plot
at 10 and 15 percent porosity
Capillary pressure, psi (mercury/air)
2000
1000
500
200
100
50
40
30
20
10
5
1
100
80
60
40
20
0
% pore volume entered by mercury
0
20
40
60
80
100
Sw%
"Average" oil
"Average" gas
1000
500
200
100
50
10
500
200
100
50
10
Height above FWL (feet)
Pore throat radius, microns

EXERCISE 10:

ESTIMATING THE DEPTH OF FREE WATER LEVEL (FWL) IN A MISSISSIPPI CHAT GAS WELL FROM LOG DATA AND CAPILLARY PRESSURE CURVES ON A PICKETT PLOT

The Mississippi "Chat" consists of tripolitic chert and provides some prolific gas reservoirs in southern Kansas. In the Glick field, porosity ranges between 26 and 51 percent (Duren, 1960). Much of this porosity is micro- in size, so that there are high water saturations held by capillary forces and low resistivities recorded on wireline logs in productive intervals. Field experience shows that zones with porosities below 15 -20% will tend to be water-filled.

The logs shown are taken from a gas well in the Glick Field and log data from four zones are tabulated below (also from Duren, 1960). Using these log data, representative capillary pressure curves measured from core samples, and a standardized Pickett plot, we will estimate the depth of the Free Water Level (FWL) in this well and the porosity cut-off for total water saturation.

For this exercise:

(1) Complete the log data below with the computation of *Rt/Rw* ratios. An *Rw* value of 0.05 ohm-m was measured at 75°F. Use the *Rw* value corrected to zone temperature that you computed in Exercise 3(i).

(2) Establish a water line on the standardized Pickett plot. Use a value of the cementation exponent, $m = 2.36$ that resulted from core measurements of formation factor in the chat.

(3) Crossplot the zone porosities and calculated *Rt/Rw* ratios on the standardized Pickett plot.

(4) Compute the resistivity index, *I*, for water saturations of 20, 30, 40, 50, 60, 70, 70, 80, and 90% water saturation using a value of n=1.8 that was measured from chat core. Remember that: $I = \frac{1}{Sw^n}$

(5) Locate water saturation lines for these values on the Pickett plot.

(6) Using the capillary pressure curves, locate gas column heights of 50, 100, 150, 200, 300, 400, and 500 feet above FWL at porosity levels of 30, 40, and 50%. Link the common height points to form gas column height contours.

(7) What is your estimate of the depth of the FWL? What do you think might be an appropriate cut-off level for porosity below which you would expect total water saturation?

Depth	F%	Rt	Rt/Rw
4838	36.6	1.7	
4846	35.0	1.6	
4856	43.4	1.15	
4866	32.8	1.7	

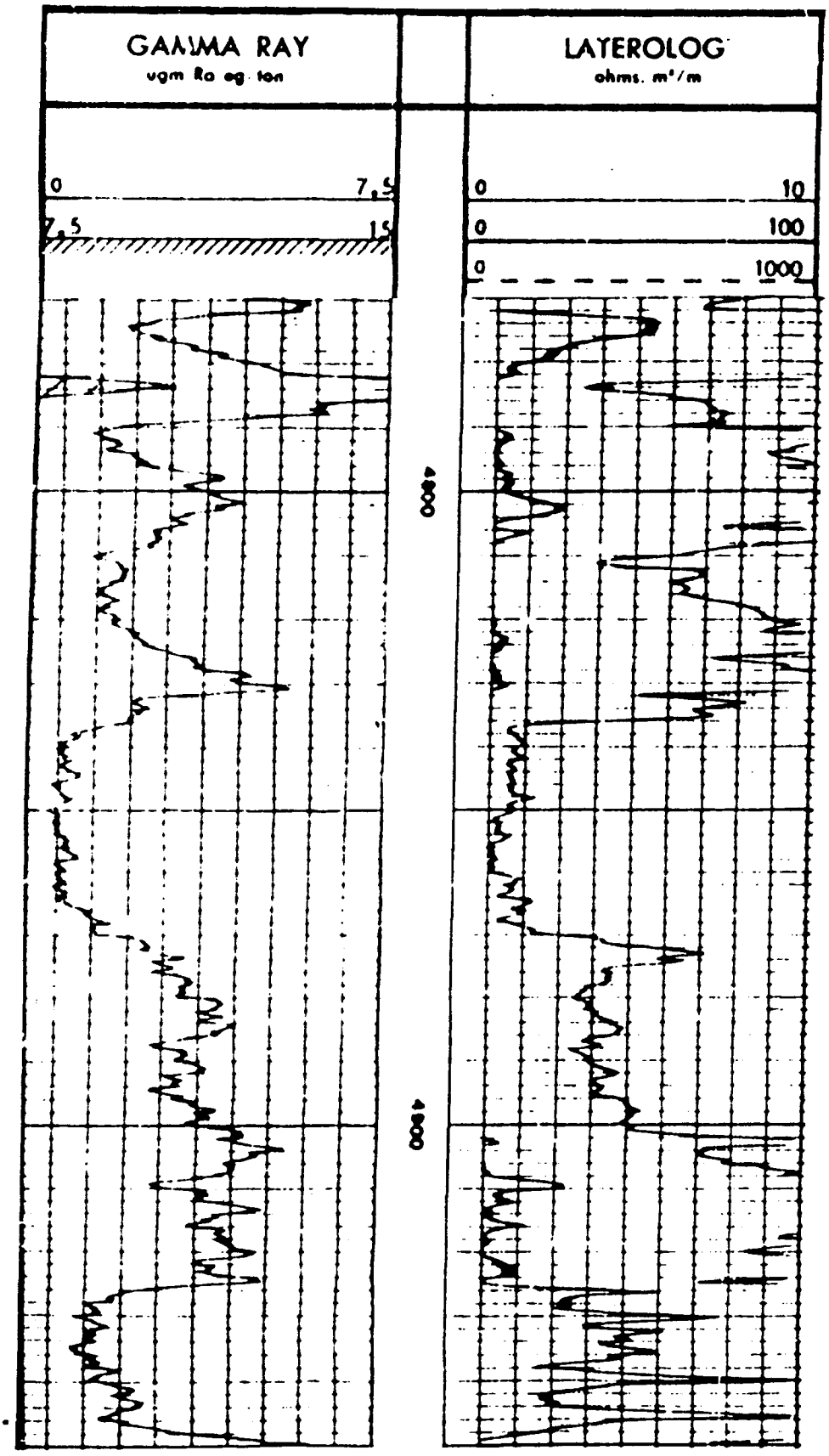

Logs from Mississippi Chat well in Glick Field, Kansas used in Exercise 9.

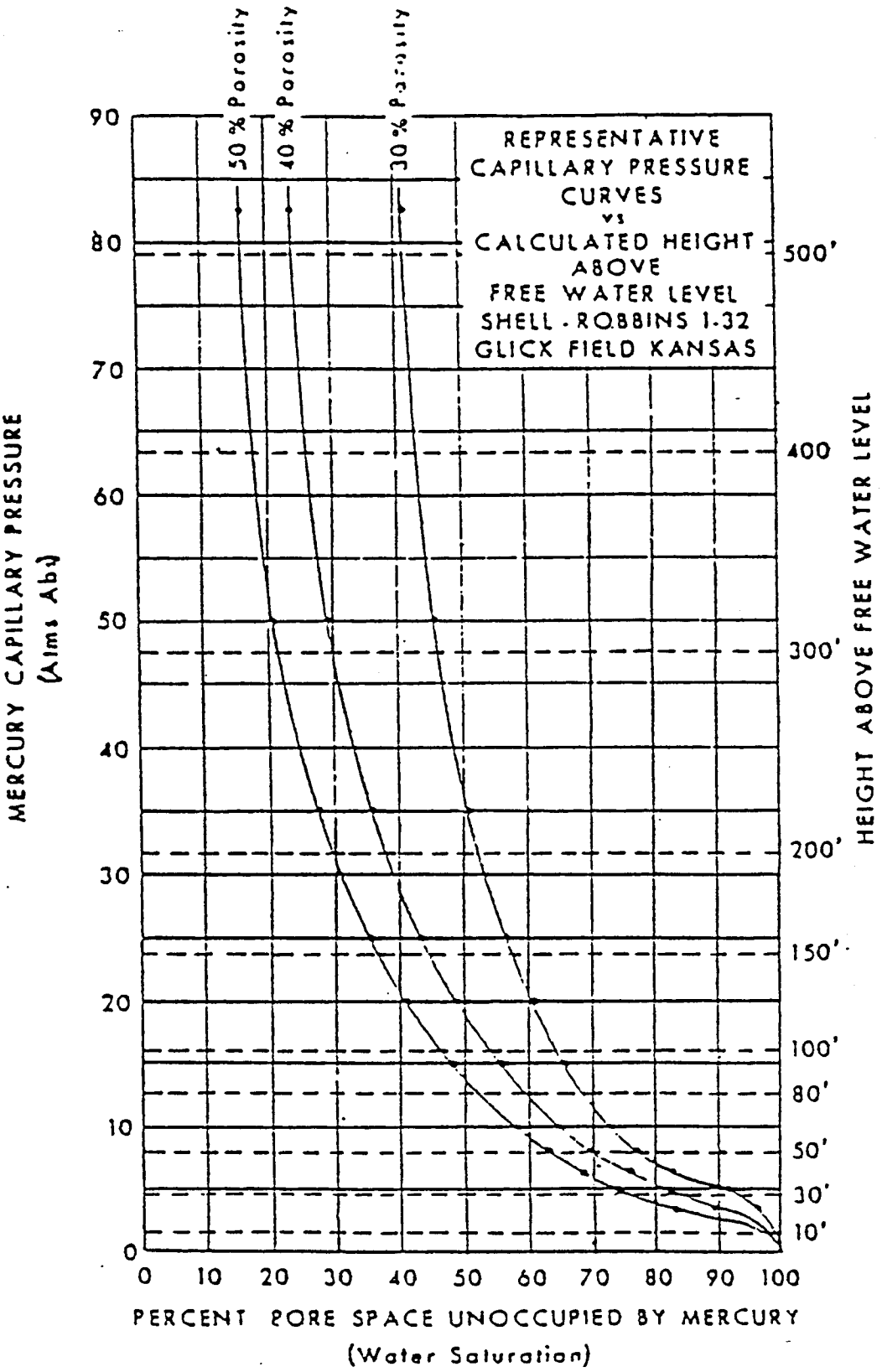

Representative capillary pressure curves of the Mississippi Chat in the Glick Field, Kansas. Note that pressure units are in atmospheres.
(from Duren, 1960)

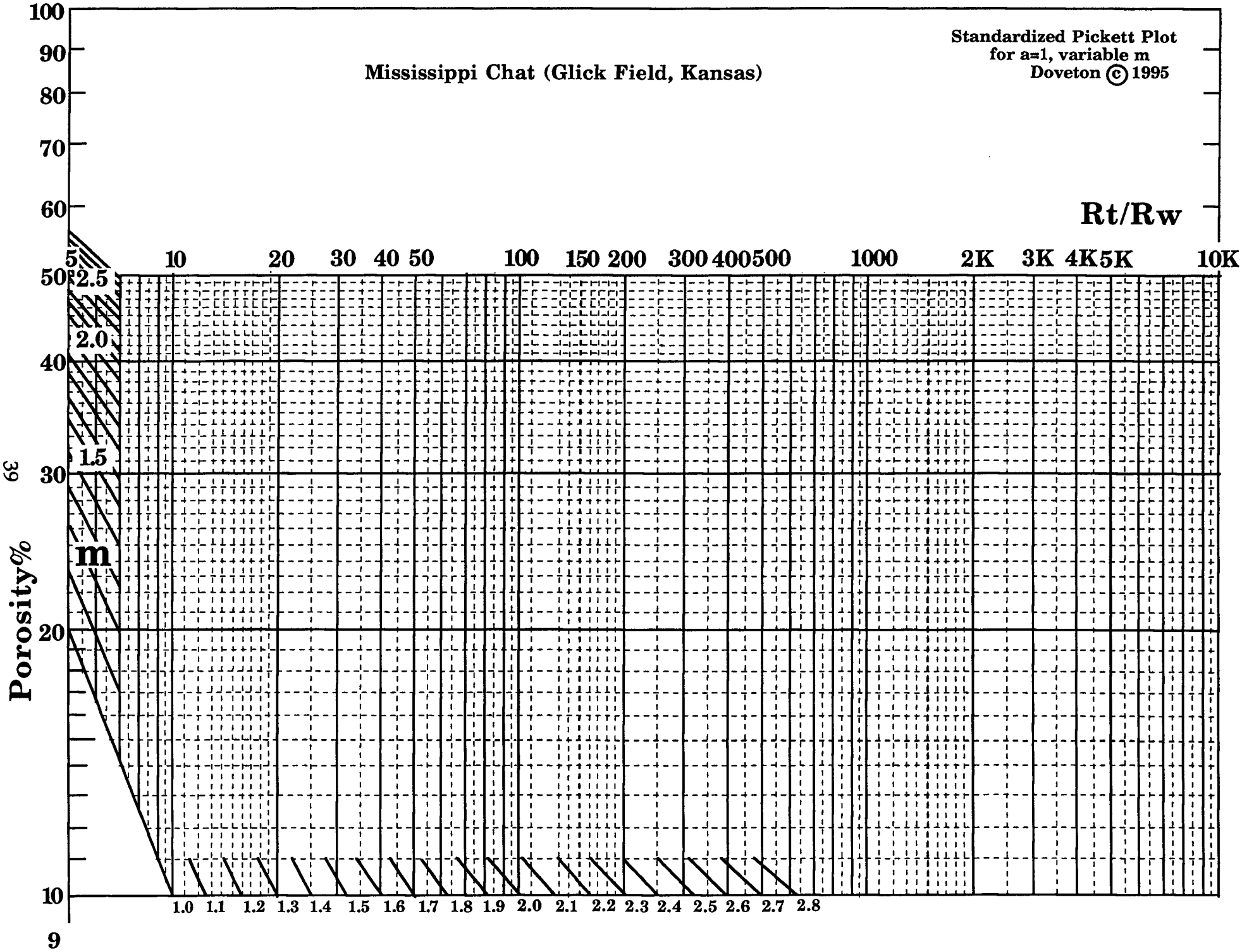
Mississippi Chat (Glick Field, Kansas)
Standardized Pickett Plot
for a=1, variable m
Doveton © 1995
Rt/Rw
5
10
20
30
40
50
100
150
200
300
400
500
1000
2K
3K
4K
5K
10K
2.5
2.0
1.5
m
Porosity%
39
100
90
80
70
60
50
40
30
20
10
9
1.0
1.1
1.2
1.3
1.4
1.5
1.6
1.7
1.8
1.9
2.0
2.1
2.2
2.3
2.4
2.5
2.6
2.7
2.8

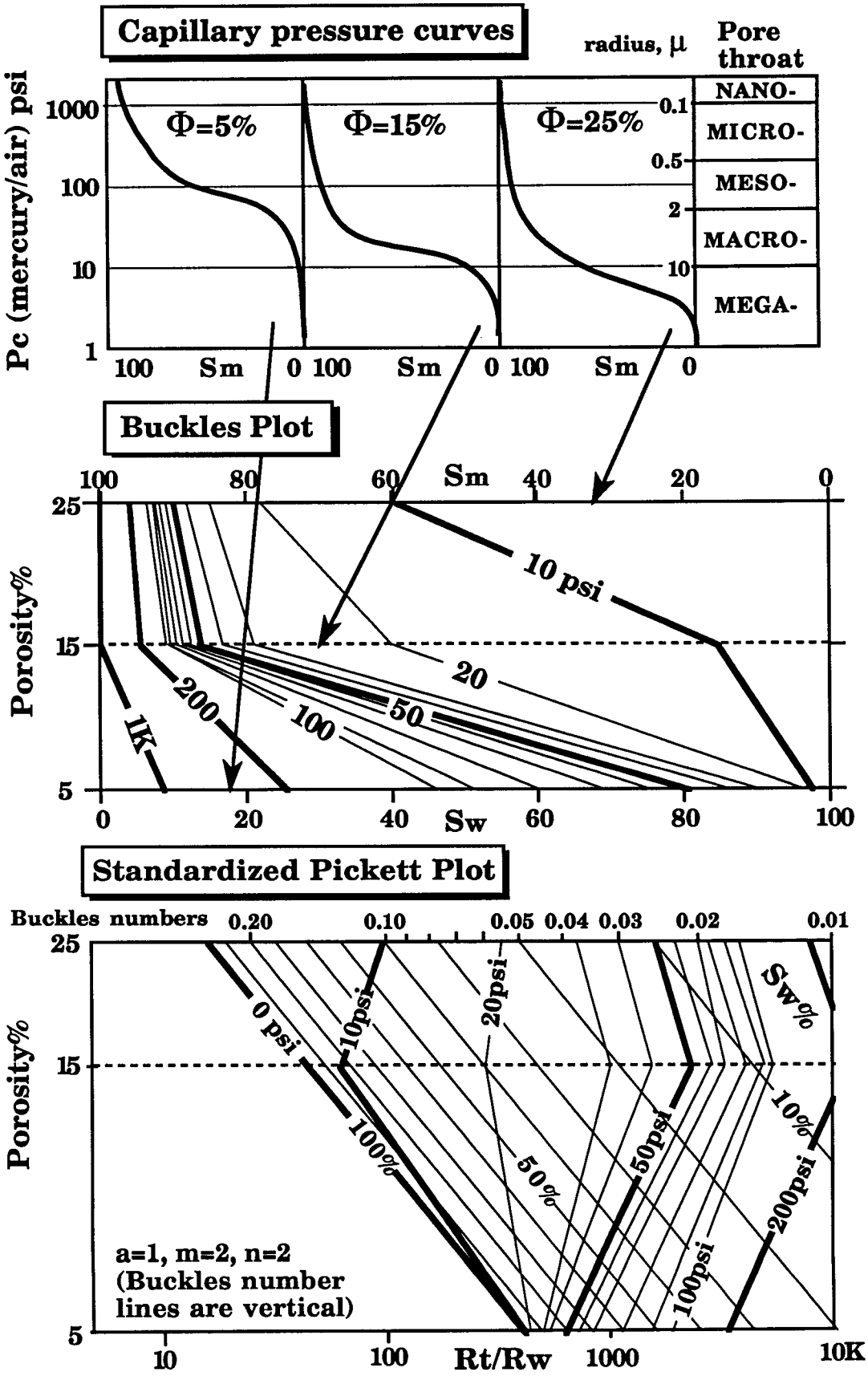

MIDDLE DEVONIAN RAINBOW REEF DOLOMITES, ALBERTA
(Data from Wardlaw, 1976)

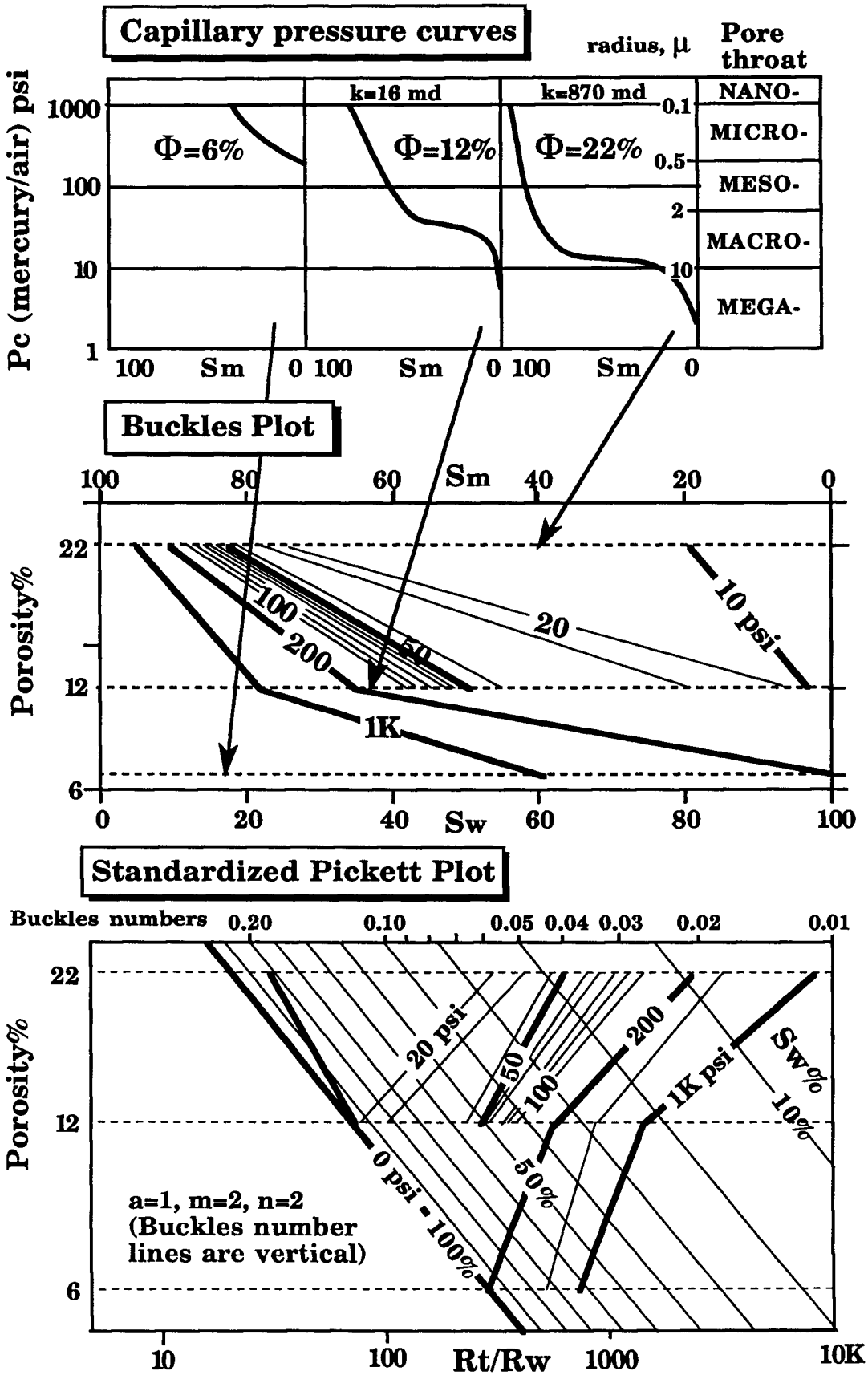

PERMIAN ROTLIEGENDES SANDSTONE, SOUTHERN NORTH SEA
(Data from Cuddy, Allinson and Steele, 1993; Hartmann, 1985)

Blank